PERI-IMPLANTITIS PROGNOSIS USING METABOLOMIC BIOMARKERS IN PERI-IMPLANT CREVICULAR FLUID: A LONGITUDINAL STUDY

A THESIS

SUBMITTED TO THE FACULTY OF THE

UNIVERSITY OF MINNESOTA

BY

HATEM ALASSY, BDS

IN PARTIAL FULFILLMENT OF THE REQUIERMENTS

FOR THE DEGREE OF

MASTER OF SCIENCE

ADVISOR: MASSIMO COSTALONGA, DMD, PhD

May 2021

ACKNOWLEDGEMENTS

I thank and acknowledge the individuals who were part of my periodontology education and specifically who were a part of this research project:

Dr. Massimo Costalonga, my advisor and mentor, for his confidence in me, guidance, and for the endless hours he tirelessly dedicated to support me throughout my residency. I am forever grateful for his instruction and trust. He remains a role model.

Dr. Larry F. Wolff for his continuous guidance, encouragement and dedication throughout my education. He is a distinguished individual.

Dr. Kim C. Mansky for her instruction, valuable support and direction through my academic journey.

Mr. Todd Rappe, at the Minnesota Nuclear Magnetic Resonance (NMR) Center, for his time and effort in the analysis of samples and guidance.

Erich Kummerfeld, Sisi Ma and Dyah Adila, for their statistical analysis of the patient demographics in this project.

The Graduate Periodontology instructors, hygienists, assistants and staff for their support throughout my academic years.

My co-residents who were and remain influential in my pursuit of knowledge, Dan Jabs, Alessandro Pedercini, Ioannis Kormas and Barbara Botorous. And for my co-residents who were a part of this project.

DEDICATIONS

I dedicate this thesis to my family and friends who supported me in my life and career. To my late father Mohamed for his years of dedication, for his unquestionable support and encouragement and for being the role model in my life. To my mother Fadila, my brother Ahmed and his son Adam for their influence in my life. To my friends who encouraged me to take the path less taken.

I dedicate this thesis to my wife, my soulmate, Natalya for her unconditional love and encouragement. For her genuine support and for her patience throughout this challenging research project. For my son Zane, the joy of my life.

ABSTRACT

Title: Peri-implantitis Prognosis Using Metabolomic Biomarkers in Peri-Implant Crevicular Fluid: A Longitudinal Study.

Background: Peri-implant diseases, peri-implantitis (PI) and peri-implant mucositis (PIM), are highly prevalent in subjects with dental implants. Despite this prevalence, diagnosing peri-implant disease (PID) remains challenging because of lack of accuracy and precision of periodontal probing and dental radiographs. Furthermore, these diagnostic tools document history of disease rather than current disease activity. There is no current model to predict the progression of PID. Biomarkers are commonly used in medicine to objectively determine disease state, or responses to a therapeutic intervention. Biomarkers in peri-implant crevicular fluid (PICF) show promise in their diagnostic and prognostic value. Metabolomic analysis of PICF quantifies molecules associated with host and bacterial metabolism may reflect on pathophysiology of peri-implantitis. Un-targeted metabolomics allows the discovery of unknown biomarkers without bias to correlate them with peri-implantitis and its progression.

Aim: We *hypothesize* that the simple metabolites in PICF are predictors of future peri-implantitis progression. We *aim* to define the unique set of metabolites in the PICF that establish a reliable method for early prediction of bone-loss progression in peri-implantitis.

Methods: Clinical and radiographic examinations and PICF samples were collected from 130 implants in 71 subjects at baseline, 6, 12, 18 and 24 months. At baseline, 59 implants were healthy (bone loss < 2mm; PD ≤ 4mm), 33 implants had PI (bone loss ≥ 3mm; PD ≥ 6mm) and 38 other implants had bone loss ≥ 2mm and <3mm and PD 5mm. Radiographic bone level changes of 112 implants and relative metabolites in PICF samples were measured at each 6 months interval using proton nuclear magnetic resonance (H-NMR) spectroscopy. MetaboAnalyst 5.0 software correlated

metabolite levels with radiographic bone changes of ≥ 1mm within a 6-month interval.

Results: In the cross-sectional component at baseline, univariate ROC curve analysis demonstrated that the Cadaverine/Lysine signature was significantly correlated with peri-implantitis (AUC= 0.76; 95% CI 0.658-0.855, p< 0.000) versus healthy implants. While alpha ketoglutarate was significantly correlated with healthy implants (AUC= 0.706; 95% CI 0.593-0.819; p= 0.002). In the longitudinal component, the metabolite levels in PICF of untreated diseased implants that demonstrated progressive radiographic bone loss of ≥ 1mm within a 6-month interval (group A, n=6) were compared to the metabolites of healthy-non-progressing implants (group B, n=26) and to diseased-non-progressing implants (group C, n=8). Proline and 1-3-diaminopropane levels could predict future bone loss of ≥ 1mm (AUC= 0.917 and 0.854 respectively) whereas glucose and arginine levels could predict the absence of bone loss in group C and group B respectively (AUC= 0.896 and 0.801) although statistical significance was not reached for all 4 metabolites. Biotin and propionate levels were higher in group C compared group A and group B (ANOVA p< 0.001; AUC_{biotin}= 0.889; $AUC_{propionate}$= 0.87). Valine levels were higher in both group A and group C compared to group B (p= 0.002; AUC= 0.841).

Conclusions: PICF metabolites identified using H-NMR spectroscopy mapped a specific metabolomic profile able to identify implants with peri-implantitis versus healthy implants with moderate accuracy. Furthermore, specific metabolites discriminated between progressive disease versus non-progressing disease status and health.

TABLE OF CONTENTS

LIST OF TABLES

LIST OF FIGURES

1. INTRODUCTION

1.1 Background

Teeth may be lost due to trauma or infectious diseases. Dental implants are one of the options to replace missing teeth (Renvert, Persson et al. 2018). There has been a significant increase in the incidence of dental implant insertions among adults in the United States by 14% per year from 1999 to 2016. Six percent of adults in the U.S. had benefited from dental implants by 2016. The dental implant prevalence among U.S. adults could reach 17% by 2026 if the trend continues at the current pace (Elani, Starr et al. 2018).

As implants are becoming more common, associated disease prevalence shows a positive correlation. Peri-implant mucositis (PIM) is defined as an inflammatory lesion of the soft tissues surrounding an endosseous implant without loss of supporting bone or continuing marginal bone loss (Heitz-Mayfield and Salvi 2018). On the other hand, peri-implantitis (PI) is a pathological condition occurring in tissues around dental implants, characterized by inflammation in the peri-implant connective tissue and progressive loss of supporting bone (Schwarz, Derks et al. 2018). According to a meta-analysis and systematic review, the estimated prevalence of peri-implantitis is 22% and peri-implant mucositis is 43% (Derks and Tomasi 2015). The absence of signs of clinical inflammation is considered peri-implant health (Araujo and Lindhe 2018).

There was a wide heterogeneity in defining peri-implantitis. Clinicians attempted to differentiate how much radiographic bone loss would be indicative of disease, as opposed to the expected post-placement bone remodeling. The current radiographic criteria for peri-implantitis is defined as bone loss of ≥ 2 mm according to the 2017 World Workshop on the Classification of Periodontal and Peri-implant Diseases and Conditions (Berglundh, Armitage et al. 2018). In the absence of initial radiographs and

probing depths, radiographic evidence of bone loss of ≥ 3 mm and/or probing depths ≥6 mm in conjunction with profuse bleeding fits the definition for PI.

The progression of PI was found to have an annual rate of bone loss of about 0.4 mm but in a non-linear and accelerating pattern (Derks, Schaller et al. 2016). Peri-implantitis often appears within the first few years after the implant is in function (Renvert, Persson et al. 2018). Plaque/biofilm is a principal etiological factor; except for some unusual factors such as implant fractures and iatrogenic errors. It has been shown that there is an increased risk of developing PI in patients who have a history of severe periodontitis, poor plaque control, and no regular maintenance care after implant therapy (Berglundh, Armitage et al. 2018).

Destructive periodontal diseases are the result of environmental, host, and bacterial factors (Wolff, Dahlen et al. 1994). Similarly, PI exhibits a chronic inflammatory response to the bacterial biofilm on the tooth/implant surface (Heitz-Mayfield and Lang 2010). PIM precedes PI and the progression of PI appears to be faster than periodontitis around natural teeth (Schwarz, Derks et al. 2018). PIM is primarily caused by a disruption of the host–microbe homeostasis at the implant–mucosa interface and is a reversible condition (Heitz-Mayfield and Salvi 2018). There is no consensus on which surgical intervention is most reliable in controlling peri-implantitis (Englezos, Cosyn et al. 2018).

No one specific or unique bacteria has been identified in patients with peri-implant disease (PID). When compared with healthy implant sites, PI was associated with higher counts of 19 bacterial species, including *Porphyromonas gingivalis* and *Tannerella forsythia* (Schwarz, Derks et al. 2018). When compared to periodontitis in natural teeth; PI was more frequently linked with opportunistic pathogens of bacterial, fungal and viral origins which points to a heterogenous infection (Schwarz, Derks et al. 2018). Some individuals are believed to be more susceptible to peri-implantitis. Current evidence indicates a potential influence of various gene polymorphisms in the pathogenesis of peri-implantitis; however, prospective clinical studies having sufficient sample size are currently lacking (Schwarz,

Derks et al. 2018). Gram-negative bacteria are the most important bacteria frequently isolated from the periodontal pockets of natural teeth, such as: *Aggregatibacter actinomycetemcomitans, Eikenella corrodens, Fusobacterium nucleatum, Prevotella intermedia, Porphyromonas gingivalis and Tannerella forsythia* (Patini, Staderini et al. 2018). However, a recent systematic review pointed out the importance of new pathogens such as: Desulfobulbus spp., Filifactor alocis and TM7 spp. in periodontal disease (Patini, Staderini et al. 2018). Notably, periodontal disease around natural teeth is not caused by the presence of specific bacteria, but by changes in the levels of different species within the oral microbiome.

The traditional clinical method to assess implant health includes a periodontal probe to measure the pocket depths and to observe bleeding upon probing. Unfortunately, this simple tool has limitations. The absence of a periodontal ligament around implants and the prosthetic design may make assessment of pocket probing depth measurements difficult to perform and interpret. Additionally, the implant mucosal seal may have less resistance to probing compared to natural teeth. This may lead to mechanically induced bleeding when probing around healthy implants. However, the healing of the epithelial attachment seems to be complete five days after clinical probing, hence, does not seem to jeopardize the longevity of implants according to an animal study (Etter, Hakanson et al. 2002). Radiographs should be standardized and compared to reference radiographs taken at the time the implant was placed in function. Furthermore, there is no practical model to predict the progression of PI (Renvert, Persson et al. 2018). Predicting disease progression is an essential component to formulate a prognosis. Treatment protocols cannot be easily compared without a valid prognosis. Non-surgical therapy of PI is often ineffective, and the treatment of choice is a surgical approach (Englezos, Cosyn et al. 2018). Surgical techniques may include open flap debridement with removal of the inflammatory tissue and mechanical and chemical decontamination of the exposed implant surface. Recontouring the bony architecture and smoothing of the implant surface may improve infection control. Regenerative procedures using a membrane and

bone graft substitutes attempting to partially fill the bony defects caused by peri-implantitis can be successful (Roccuzzo, Layton et al. 2018). Therapy of peri-implantitis followed by regular supportive care resulted in favorable clinical improvements and stable peri-implant bone levels in the majority of patients according to a systematic review (Sahrmann, Attin et al. 2011).

The early diagnosis of PID and its rate of progression are a great challenge. Assessment of biomarkers may aid in the early detection of PI. Biomarkers may assist both in staging and grading of periodontitis in the case definition system of periodontitis (Tonetti, Greenwell et al. 2018). Peri-implant crevicular fluid (PICF), also described as peri-implant sulcular fluid (PISF), may contain biomarkers to diagnose and predict future disease which aids in choosing a specific treatment protocol. A biomarker is a parameter that is objectively measured and evaluated as an indicator of normal biological, pathogenic processes, or responses to a therapeutic intervention (Strimbu and Tavel 2010). Molecules in the gingival crevicular fluid (GCF) collected from natural teeth have been extensively studied. Substances such as lactate dehydrogenase and myeloperoxidase have been investigated to determine if they could be used as markers for periodontal pathology and in the success of treatment modalities (Wolff, Smith et al. 1988). Another approach was described in a recent report which found that measuring glycosylated hemoglobin in gingival crevicular *blood* was successfully used to screen for diabetes control in a dental office setting (Kim, Wolff et al. 2015). Most of the PI biomarker studies focused on pro-inflammatory cytokines, enzymes and bone metabolism proteins (Ma, Kitti et al. 2000, Ma, Kitti et al. 2003, Arikan, Buduneli et al. 2008, Schierano, Pejrone et al. 2008, Arikan, Buduneli et al. 2011, Zani, Moss et al. 2016). Table 1 lists keywords and abbreviations in this manuscript.

Table 1. Keywords and abbreviations

PI	Peri-Implantitis
PIM	peri-implant mucositis
PID	peri-implant disease
GCF	Gingival crevicular fluid
PICF	peri-implant crevicular fluid
MMP	matrix metalloproteinase
IL-1β	Interleukin 1 beta
IL-6	Interleukin-6
IL-1ra	interleukin-1 receptor antagonist
TNFα	tumor necrosis factor alpha
GM-CSF	granulocyte-macrophage colony-stimulating factor
MIP-1α	macrophage inflammatory protein-1α
RANK	receptor activator of nuclear factor kappa-B
RANKL	receptor activator of nuclear factor kappa-B ligand
sRANKL	soluble Receptor activator of nuclear factor kappa-B ligand
OPG	osteoprotegerin
TIMP	tissue inhibitor of metalloproteinases
MPO	myeloperoxidase
tPA	tissue plasminogen activator
TRAP	tartrate-resistant acid phosphatase
CatK	cathepsin K
PAI	plasminogen activator inhibitor
VEGF	vascular endothelial growth factor
ICTP	C-telopeptide pyridinoline cross linkage of type I collagen
α-KG	Alpha ketoglutarate
ELISA	enzyme-linked immunosorbent assay
AUC	area under the curve (receiver operating characteristic)

2. LITERATURE REVIEW

2.1. Gingival crevicular fluid & peri-implant crevicular fluid in health and disease

GCF is a physiological fluid and an inflammatory exudate originating from the gingival plexus of blood vessels in the gingival corium, subjacent to the epithelium lining of the dentogingival space. GCF flows through the external basement membrane and the junctional epithelium to reach the gingival crevice. The composition of GCF can potentially be used to detect subclinical alterations in tissue metabolism, inflammatory-cell recruitment and connective tissue remodeling (Barros, Williams et al. 2016). Cytokines and enzymes located in the gingival tissues may lead to the degradation of connective tissue collagen and alveolar bone. These are host response factors from local host tissue reacting to the plaque biofilm. In the presence of disease, the volumes of GCF and PICF were similarly higher than in healthy sites, and GCF flow increases with an increase in the severity of gingival inflammation (Bevilacqua, Biasi et al. 2016). Significant positive correlations were noted between the concentrations of cytokines in PICF versus their levels in GCF around natural teeth (Recker, Avila-Ortiz et al. 2015). Another study compared the cytokine and bacterial levels from around implants versus teeth within the same individual (Gurlek, Gumus et al. 2017). There were many similarities but, also some differences in levels of IL-1β and soluble receptor activator nuclear factor kappa-B ligand (sRANKL) and bacterial species between peri-implant and periodontal sites in the same individuals, suggesting similar pathogenic mechanisms. Investigators compared crevicular fluid from diseased teeth and implants, and tested collagenase activity and collagenolytic matrix metalloproteinase (MMP) levels. Results indicated that peri-implantitis PICF contained higher active MMP-8 levels than GCF from similarly deep chronic periodontitis sites of natural teeth (Xu, Yu et al. 2008). A 10-year retrospective investigation comparing crevicular fluid biomarkers from implants and teeth concluded that increased levels of MMP-8 and IL-1β in PICF or GCF may be associated with inflammation around implants and

teeth while lower levels of MMP-1/TIMP-1 may be an indicator of disease progression around implants (Ramseier, Eick et al. 2016).

2.2. PICF disease mediators (Cytokines)

The gingival sulcus forms a unique ecological niche for microbial colonization. As the salivary film transitions at the crown to the gingival sulcus, its composition changes and the proportion of serum proteins increases due to the proximity with the crevicular fluid. The microbiota of the dental plaque biofilm drives the inflammatory process. The microbial biofilm in the gingival sulcus elicits inflammation in the surrounding connective tissue (Costalonga and Herzberg 2014). The imbalance between the bacterial challenge and host response at the soft tissue–implant interface triggers an inflammatory process (Wang, Garaicoa-Pazmino et al. 2016). Cytokines, such as Tumor necrosis factor alpha (TNFα), Interleukin-1-beta (IL-1β) and Interleukin-6 (IL-6) are released from cells of the gingival epithelium, dendritic cells, connective tissue fibroblasts, macrophages and neutrophils. In addition, a number of enzymes, such as matrix metalloproteinases, are produced by neutrophils, fibroblasts and osteoclasts, leading to the degradation of connective tissue collagen and alveolar bone (Barros, Williams et al. 2016). More than 90 different molecular components in GCF have been evaluated for potential periodontal disease diagnosis associated with the natural dentition (Loos and Tjoa 2005). To date, significantly fewer PICF components have been analyzed around implants.

PI and periodontitis lesions exhibit critical histopathologic differences, which contribute to the understanding of dissimilarities in onset and progression between the two diseases (Carcuac and Berglundh 2014). Histologically, PI lesions extend apical to the junctional epithelium and contain large numbers and densities of plasma cells, macrophages and neutrophils. PI lesions are larger than those found at PIM sites (Berglundh, Armitage et al. 2018). In contrast to periodontitis, PI lesions are more than twice the size and contain a significantly larger area, numbers, and densities of Syndecan-1 $(CD138)^{+}$, scavenger receptor class D – member 1 $(CD68)^{+}$, and

mieloperoxidase (MPO)$^{+}$ cells. Furthermore, larger densities of vascular structures are seen in the connective tissue area lateral to the infiltrated connective tissue than within the infiltrate in PI lesions (Carcuac and Berglundh 2014).

2.3. PICF research in peri-implantitis: Methods of sampling and analysis

A variety of methods have been used to sample and analyze components of PICF to diagnose PI. The most common method used to collect PICF has been paper strips inserted into the crevice for typically 30 seconds. PICF is then absorbed onto the strips. After elution from the strips into a buffer or diluent, the fluid is evaluated utilizing biomarker-specific assays. Studies have also used paper cones, membranes and microcapillary pipettes to collect PICF.

The PICF volume is dependent upon the level of inflammation and pocket depth. The quantity of components collected in a deep and inflamed pocket would in all likelihood be higher than in healthy sulci. The concentration versus the quantity of the collected PICF components may offer more value in the search of valid biomarkers; however, this may be controversial (Chatzopoulos, Mansky et al. 2019). Enzyme-linked immunosorbent assay (ELISA), flow cytometry, Luminex and Spectrophotometry were the most utilized assays in PICF research. Typically, studies used ELISA to analyze PICF and evaluated one to two cytokines (Duarte, Serrao et al. 2016).

2.4. Analysis of the current literature on PICF biomarkers

2.4.1. PICF molecules investigated

Most PI biomarker studies analyzed the correlation of enzymes and cytokines between healthy and diseased implants. Such components include proinflammatory cytokines such as TNFα, IL-1β, IL-6, IL-17 and anti-inflammatory cytokines such as IL-10 (Schierano, Pejrone et al. 2008, Duarte, de Mendonca et al. 2009, Casado, Canullo et al. 2013, Wohlfahrt, Aass et al. 2014, Faot, Nascimento et al. 2015, Zani, Moss et al. 2016, Gurlek, Gumus et

al. 2017). Other cytokines analyzed were interleukin-1 receptor antagonist (IL-1ra) and Granulocyte-macrophage colony-stimulating factor (GM-CSF) (Zani, Moss et al. 2016). Some studies investigated chemokines such as IL-8 and macrophage inflammatory protein-1α (MIP-1α) (Hall, Pehrson et al. 2015, Bhavsar, Miller et al. 2019). Other reported investigations analyzed bone metabolism markers such as Receptor activator nuclear factor kappa-B ligand (RANKL), Receptor activator nuclear factor κ B (RANK), Osteoprotegerin (OPG) and Osteocalcin (Monov, Strbac et al. 2006, Arikan, Buduneli et al. 2008, Arikan, Buduneli et al. 2011, Rakic, Lekovic et al. 2013, Dursun and Tozum 2016, Cakal, Efeoglu et al. 2018). Other trials investigated enzymes such as matrix metalloproteinases (MMP1, MMP8, MMP9, MMP13), tissue inhibitor of metalloproteinases 1&2 (TIMP) (Ma, Kitti et al. 2000, Ma, Kitti et al. 2003, Sorsa, Tervahartiala et al. 2011, Arakawa, Uehara et al. 2012, Basegmez, Yalcin et al. 2012, Wohlfahrt, Aass et al. 2014, Ramseier, Eick et al. 2016, Ghassib, Chen et al. 2019), Elastase, Myeloperoxidase (MPO) (Dursun and Tozum 2016), tissue plasminogen activator (tPA), tartrate-resistant acid phosphatase (TRAP), cathepsin K (CatK) (Strbac, Monov et al. 2006, Yamalik, Gunday et al. 2012, Hall, Pehrson et al. 2015, Dursun and Tozum 2016). Some authors reported on other PICF components such as plasminogen activator inhibitor 2 (PAI-2), vascular endothelial growth factor (VEGF), prostaglandin E2, KLIKK-protease genes and miropin (Hall, Pehrson et al. 2015, Dursun and Tozum 2016, Zani, Moss et al. 2016, Eckert, Mizgalska et al. 2018). A summary of commonly investigated PICF biomarkers in peri-implantitis is shown in **Table 2.**

Table 2. Summary of commonly investigated peri-implant crevicular fluid (PICF) biomarkers in peri-implantitis.

Biomarker	Summary	References
Cytokines:		
TNFα	higher levels in diseased vs healthy implants	(Duarte, de Mendonca et al. 2009, Faot, Nascimento et al. 2015, Zani, Moss et al. 2016, Ghassib, Chen et al. 2019)
IL-1β	higher levels in diseased vs healthy implants	(Panagakos, Aboyoussef et al. 1996, Murata, Tatsumi et al. 2002, Schierano, Pejrone et al. 2008, Casado, Canullo et al. 2013, Hall, Pehrson et al. 2015, Ramseier, Eick et al. 2016, Wang, Garaicoa-Pazmino et al. 2016, Gurlek, Gumus et al. 2017, Ghassib, Chen et al. 2019)
IL-10	negative correlation with diseased implants	(Casado, Canullo et al. 2013, Zani, Moss et al. 2016)
Bone markers:		
sRANKL, RANK, OPG	mixed results or no correlation between biomarker and PID	(Monov, Strbac et al. 2006, Arikan, Buduneli et al. 2008, Arikan, Buduneli et al. 2011, Rakic, Lekovic et al. 2013)
Osteocalcin	mixed results or no correlation between biomarker and PID	(Dursun and Tozum 2016, Cakal, Efeoglu et al. 2018)
Enzymes:		
MMP-1	higher levels in diseased vs healthy implants	(Nomura, Ishii et al. 2000)
MMP-8	higher levels in diseased vs healthy implants	(Ma, Kitti et al. 2000, Nomura, Ishii et al. 2000, Sorsa, Tervahartiala et al. 2011, Arakawa, Uehara et al. 2012, Basegmez, Yalcin et al. 2012, Wohlfahrt, Aass et al. 2014, Ramseier, Eick et al. 2016, Ghassib, Chen et al. 2019)

MMP-9	higher levels in diseased vs healthy implants	(Ma, Kitti et al. 2003)
MMP-13	higher levels in diseased vs healthy implants	(Ma, Kitti et al. 2000)
Myeloperoxidase	higher levels in diseased vs healthy implants	(Dursun and Tozum 2016)
Elastase	higher levels in diseased vs healthy implants	(Dursun and Tozum 2016)
Cathepsin K (CatK)	higher levels in diseased vs healthy implants	(Strbac, Monov et al. 2006, Yamalik, Gunday et al. 2012, Hall, Pehrson et al. 2015, Dursun and Tozum 2016)

2.4.2. Proinflammatory cytokines

Most investigations including systematic reviews and meta-analyses focused on the assessment of proinflammatory cytokines IL-1β and TNFα levels, demonstrating that PI sites were associated with a significant increase in their levels compared to healthy implants. IL-1β and TNFα are the two most important cytokines in osteoclast formation and bone resorption. IL-1β is mainly produced in macrophages and regulates the degradation of extracellular matrix components of the plasminogen system and collagenase activity in inflammation and wound healing. It has been shown that inhibition of IL-1β reduces tissue breakdown and the progression of tissue inflammation (Delima and Van Dyke 2003). TNFα induces fibroblast apoptosis and reduction of the repair capacity of peri-implant tissue (Faot, Nascimento et al. 2015). Statistical differences were revealed when IL-1β and TNFα levels were compared between healthy implant sites and PID sites. No statistical differences could be detected between PIM and PI (Faot, Nascimento et al. 2015). There is limited evidence presented in published literature that other proinflammatory cytokines (IL-6 and IL-17) have higher levels in PI compared to crevicular fluid associated with healthy implants (Wohlfahrt, Aass et al. 2014, Zani, Moss et al. 2016). Contrary to what was found with IL-1β, IL-6 increases significantly between PIM and PI. IL-1β yielded a significant increase after 3 weeks of cessation of oral hygiene measures and was reversed to pre-experimental levels 69 days after oral hygiene measures were reinstated (Schierano, Pejrone et al. 2008). IL-6 links innate and acquired immune responses, in which it induces differentiation of activated B cells into antibody-producing cells as well as naïve CD4+ T cells into IL-17 expressing T cells when TGF-β is also present (Ghassib, Chen et al. 2019). Studies of experimental PIM demonstrated that TNFα and TGF-β2 levels did not change during an experimental PIM period. IL-1β, VEGF, and TIMP-2, *T. denticola* and *Prevotella intermedia* showed diagnostic validation for PI in this study. IL-1β demonstrated the most significant ability for the prediction of PI disease status (sensitivity: 0.73, specificity: 0.73, odds ratio: 7.71) which is a moderate level of accuracy. The authors concluded that a combination of the above

markers and microbial profiles may offer site-specific diagnosis of PID due to the increased sensitivity and specificity compared to individual biomarkers (Wang, Garaicoa-Pazmino et al. 2016). To summarize, higher IL-1β and TNFα levels within the PICF was found to be associated with diseased compared to healthy implants. While combining cytokines and other molecules improved the accuracy to differentiate healthy from diseased implant sites, the confidence remained moderate.

2.4.3. Anti-inflammatory cytokines and chemokines

IL-10 in PICF has been shown to be negatively correlated with peri-implant disease (Casado, Canullo et al. 2013, Zani, Moss et al. 2016). IL-4 and IL-8 showed no differences between health and PID (Duarte, Serrao et al. 2016). Chemokines IL-8 and Macrophage inflammatory protein-1α (MIP-1α) were higher in diseased sites (Hall, Pehrson et al. 2015, Bhavsar, Miller et al. 2019).

2.4.4. Bone loss markers

Since RANKL and OPG are key factors regulating bone metabolism, it is likely they are involved in alveolar bone destruction in PI (Arikan, Buduneli et al. 2008). However, the majority of studies failed to identify any significant differences in the levels of bone metabolism markers between healthy and PI sites (Dursun and Tozum 2016). Soluble RANKL and OPG levels were evaluated in 84 samples of PICF from implants showing different peri-implant tissue clinical conditions without demonstrating any correlation between these levels and the studied clinical outcomes (Monov, Strbac et al. 2006).

However, one study demonstrated the presence of OPG in 79% of the PICF samples and showed a significant positive correlation between BOP, while sRANKL was only detected in 12% of PICF samples and did not show any positive correlation with clinical inflammation (Arikan, Buduneli et al. 2008). Another study compared the levels of C-telopeptide pyridinoline cross linkage of type I collagen (ICTP), sRANKL and OPG in PICF (Arikan, Buduneli et al. 2011). The results demonstrated “an increase in total amount of ICTP

and OPG in the PI group when compared to the healthy group. However, sRANKL was not significantly different between the healthy implant and diseased implant groups". Alternatively, another report showed "significantly higher levels of sRANKL, OPG and RANK in PI sites compared to healthy implant sites" (Rakic, Lekovic et al. 2013). However, OPG/sRANKL ratio demonstrated no significant difference between the healthy and diseased implant groups. Osteocalcin, osteopontin and osteonectin proteins are related to bone remodeling. There were no significant differences in PICF osteocalcin, osteopontin and osteonectin total amounts between healthy controls, peri-implant mucositis and peri-implantitis groups in one recent study (Cakal, Efeoglu et al. 2018).

An interventional trial assessed the effects of mechanical anti-infective therapy on the levels of TNFα and OPG/RANKL ratio in healthy implant and PI sites (Duarte, de Mendonca et al. 2009). The results demonstrated significantly higher levels of TNFα in PI sites when compared to healthy sites. OPG/RANKL ratio was shown to be low in healthy sites compared to PI sites. After mechanical anti-infective therapy, TNFα levels were significantly reduced in treated diseased sites and reached the same level as in healthy control sites at 3 months post therapy. In summary, bone metabolism markers in PICF cannot reliably differentiate healthy vs diseased implants.

2.4.5. Enzymes

Certain enzymes in PICF, such as cathepsin K and MMPs, were heavily investigated. Cathepsin-K (CatK) is a cysteine protease that is highly expressed by osteoclasts. Its main function is hydrolyzing the extracellular bone matrix proteins. CatK was shown to be elevated in GCF from chronic periodontitis sites compared to healthy sites. CatK is a known marker of bone turnover due to its key role in remodeling and cartilage breakdown in bone by hydrolyzing extracellular bone matrix proteins. CatK is highly and quite selectively expressed in active, resorbing osteoclasts (Almehmadi and Alghamdi 2018). This suggests its role in the pathogenesis of PI. CatK levels were evaluated in PICF to assess the levels of CatK in healthy implants and

PI in order to correlate these findings with clinical parameters. Some investigations showed a positive correlation between clinical parameters of PI and levels of CatK (Strbac, Monov et al. 2006, Yamalik, Gunday et al. 2012) while others concluded that CatK showed no differences between the healthy and diseased implant groups (Hall, Pehrson et al. 2015).

MMP upregulation has been associated with irreversible peri-implant connective tissue destruction (Dursun and Tozum 2016). One suggested reason for MMP upregulation is polymorphism in the promoter region of MMP-8 which explains varied responses between different individuals who have the same disease category (Ghassib, Chen et al. 2019). During the initiation and course of inflammatory responses in PI, proinflammatory mediators including MMP-8 are up-regulated in affected tissues and present in PICF (Sorsa, Tervahartiala et al. 2011). IL-1β and TNFα both induce the synthesis and secretion of MMP-8, which in turn, cleaves the triple helix of collagen and collectively degrade the extracellular matrix (Ghassib, Chen et al. 2019). Similar to what was found in periodontitis, there is moderate evidence in the literature showing high MMP-8 levels in PI compared to healthy implant sites (Ma, Kitti et al. 2000, Arakawa, Uehara et al. 2012, Basegmez, Yalcin et al. 2012, Ramseier, Eick et al. 2016, Ghassib, Chen et al. 2019). MMP-8 is a promising biomarker as an early signal of peri-implant inflammation (Basegmez, Yalcin et al. 2012).

Another investigation reported a positive correlation between MMP-8, PI, and BOP in both GCF and PICF (Ramseier, Eick et al. 2016). The authors concluded that “increased levels of MMP-8 and IL-1β in PICF or GCF may be associated with inflammation around teeth and implants. Other clinical trials demonstrated that MMP-8, MMP-9 and MMP-13 (also known as Collagenase-2, Gelatinase B and collagenase-3, respectively) in PICF were associated with more bone loss around diseased implants indicating that MMP-8 could be a promising biomarker for peri-implant osteolysis” (Ma, Kitti et al. 2000, Ma, Kitti et al. 2003). However, a different trial concluded that MMP-8 did not reveal a meaningful difference to differentiate PI from healthy implants (Wang, Garaicoa-Pazmino et al. 2016). A summary of the commonly investigated and

promising peri-implant crevicular fluid biomarkers are shown in **table 2**. In conclusion, MMP-8 is commonly investigated in PICF and high levels of this enzyme may be useful in the diagnosis of peri-implantitis, however, the literature includes contradictory reports and further research is needed.

2.5. PICF biomarkers: Chair-side diagnostic tests, Limitations

2.5.1. Chair-side diagnostic tests

If a definitive diagnosis for PI or PIM can be made using a test with high validity, then a reasonable question would be, if the test is feasible and if the test can predict progressive PI. Clinicians seek an easy, accurate, inexpensive and time effective test. Most diagnostic tests in dentistry are performed in a clinical setting at the dental chair. A chair-side test for the diagnosis of PID would also be valuable if it can predict the risk of disease progression at an implant site.

2.5.2. Limitations of studies

(A) Lack of a Standardized Definition of Peri-Implantitis.

The conflicting results of the above studies may be due to differences in study design, material and methods utilized, such as sample collection, processing and assay sensitivity. Meta-analyses in PICF biomarkers are scarce due to heterogeneity between studies in PI diagnosis criteria. The 2017 World Workshop hopes to utilize their PI definition criteria in future clinical and research settings (Renvert, Persson et al. 2018). If some studies set their PI definition as radiographic bone loss of 3 mm while other studies had a 2 mm cut off, then the PICF results of these investigations may not be accurately combined and analyzed. There is a wide range of different definitions regarding peri-implant mucositis and peri-implantitis that were employed in the included investigations. The definition of peri-implantitis varied over time, mainly from more permissive to stricter inclusion criteria. In the light of the new definition of peri-implantitis by the 2017 World Workshop (Berglundh, Armitage et al. 2018, Renvert, Persson et al. 2018), some of the reviewed studies may have included cases of peri-implant mucositis in the group of peri-implantitis. Such misdiagnosis of peri-implantitis and inclusion of cases of peri-implant mucositis may affect the results of studies on PICF.

(B) Predictive Value of Biomarkers

The majority of PICF studies assessed only a few cytokines, enzymes or pathogens to correlate them with peri-implant diseases. Most studies lacked data on sensitivities and specificities to biomarkers in PICF; hence the probability of false positive or false negative results could not be calculated. PICF biomarkers analyzed individually have shown mixed results or low sensitivity and high specificity values, which may weaken the biomarker's disease predictive value. On the other hand, biomarkers of periodontal disease progression in GCF alone (MMP-8, MMP-9, Osteoprotegerin, C-reactive Protein and IL-1β) provided low sensitivity and high specificity values of 23% and 95%, respectively (Kinney, Morelli et al. 2014). It is noteworthy that, combined with plaque pathogens, GCF biomarkers demonstrated the highest positive and negative predictive values of 73% and 70%, respectively (Kinney, Morelli et al. 2014). Similarly, selected PICF-derived biomarkers of periodontal tissue inflammation, matrix degradation/regulation, and alveolar bone turnover/resorptive molecules combined with a site-specific microbial profile may be used to diagnose peri-implant diseases (Wang, Garaicoa-Pazmino et al. 2016). Another multi-biomarker approach presented a 3-biomarker model (IL-17, IL-1ra and VEGF) distinguishing healthy implant PICF from PID subjects with high validity (AUC: 0.90) (Zani, Moss et al. 2016).

(C) Potential Confounders Were Not Segregated

Some reports failed to discuss important data, such as the general periodontal health in their subjects, smoking habits, systemic confounders, and other related criteria which may influence the levels of cytokines in PICF. Smoking may be an important confounder because it may affect the PICF volume and cytokine levels. Only a few studies excluded smokers. Other potential confounders may include a history of periodontitis and gingival phenotype. A retrospective study that analyzed risk factors for PID identified three predictors for PIM: history of treated periodontitis, absence of regular supportive peri-implant maintenance, and use of a bone graft (Atieh, Pang et al. 2019). The same investigation also identified three predictors for PI:

smoking, absence of regular supportive peri-implant maintenance and placement of ≥2 implants.

(D) Sampling Techniques Were Not Standardized

Standardization of PICF sampling is relevant due to the atypical morphology of the implant prosthesis. The insertion of different paper strips, cones, membranes or other devices would be technique sensitive and may offer misleading results. Biomarker concentration in the collected PICF may be adjusted for the collected volume due to the higher volume in inflamed tissues. This controversial confounder was rarely discussed in PICF studies.

(E) Longitudinal Studies Were Lacking

Biomarkers are not necessarily present in a single moment of PICF collection due to several systemic or local factors. Most studies were cross-sectional which leads to another limitation. Due to a cyclic progression of peri-implant diseases, the immune-inflammatory event biomarkers responsible for tissue breakdown may not always be active in cross-sectional studies with a single moment of fluid collection Dursun and Tozum (2016). Thus, studies on bone markers are often inconclusive despite bone loss is one of the main features of peri-implantitis. Very few longitudinal studies sampled implants over time. Some were intervention trials, sampling the diseased implants before and after therapy. Results showed that clinically stable treatment outcomes of peri-implantitis are associated with lower levels of putative pathogens total bacterial load and with reduction of IL-1β, IL-6, and VEGF levels in PICF (Renvert, Widen et al. 2017). Longitudinal studies may confirm the concentrations of biomarkers at specific sites and would theoretically show the shifts of such concentrations in diseased implants over time. These longitudinal investigations may aide in presenting biomarkers that predict the shift from health to disease or predicting the deterioration of a diseased implant. The validity of predicting PID is still in its infancy.

In summary, limitations of past studies include: (1) lack of a homogenous definition of peri-implant health and disease, (2) lack of discussions on the predictive value of biomarkers, lack of segregation of potential confounders such as systemic diseases, smoking and a history of periodontitis, (3) different

sampling techniques and (4) the lack of longitudinal studies that sampled PICF over time.

2.6. Omics; diagnosis and prediction of future disease progression

2.6.1. Proteomics and Metabolomics

The protein composition of GCF may reflect the pathophysiology of periodontal diseases. Protein profiles of GCF obtained from healthy individuals may potentially serve as a reference for identification of biomarkers of periodontal diseases by proteome analyses (Barros, Williams et al. 2016). The same may be attempted for peri-implant disease and health. A recent report demonstrated that a specific PICF proteomic profile associates with active peri-implantitis process and implant loss compared to the proteomic profile of healthy implants (Esberg, Isehed et al. 2019).

Omics involves the characterization of biomolecules and includes fields such as genomics, epigenomics, transcriptomics, proteomics, and metabolomics. Multi-omics may integrate several of these methods to reach a more definitive analysis of complex biological processes. This can pin-point relevant biomarkers which may be used to define disease and physiology. The multi-omics approach showed that “a combination of data types (marker gene analysis, metagenomics, and metabolomics) provided rich and complementary insights into the analysis of chronic periodontal disease around natural teeth” (Califf, Schwarzberg-Lipson et al. 2017). Future directions may utilize the multi-omics approach to identify biomarkers in PI. However, to our knowledge, there are no studies demonstrating metabolomic research in peri-implant disease or physiology.

Metabolomic analysis (a comparative analysis of metabolome levels between samples) that measure small degradation molecules associated with host and bacterial metabolism show promise (Barros, Williams et al. 2016). Metabolite functions include metabolism and energy storage, as well as other functions in cell-to-cell signaling, metal acquisition, and virulence (Vinayavekhin, Homan et al. 2010, Vinayavekhin and Saghatelian 2010). Mass spectrometry and nuclear magnetic resonance spectroscopy can be used to both identify and quantify chemicals from complex mixtures such as PICF. This particular approach is now being exploited to characterize the

metabolomes of many different biological samples in what is called quantitative metabolomics or targeted metabolic profiling (Wishart 2008). Metabolomics offers unique insights into small molecule regulation and signaling in biology. Cancer-specific signatures have been shown to be embedded in saliva metabolites (Sugimoto, Wong et al. 2010). Identification of a molecular signature for periodontitis using unbiased metabolic profiling could allow identification of biomarkers to assist in the diagnosis and monitoring of periodontal disease (Barnes, Kennedy et al. 2014). Untargeted metabolomics is the relative quantitation of a broad range of metabolites, both known and unknown, in different samples (Vinayavekhin, Homan et al. 2010, Vinayavekhin and Saghatelian 2010). This untargeted approach allows the discovery of unknown biomarkers without bias (the need to choose a certain substance beforehand) to correlate it with PI. These potential biomarkers may be investigated in longitudinal trials which can assist in the prediction of future disease progression.

The metabolome consists of the final products of metabolic activities within a living system. These molecules belong to different compound classes, such as amino acids, peptides and organic acids. The goal of metabolomics is to map the specific metabolites which are unique for each condition in a living system. The concentrations of these metabolites are the result of the process of gene expression, protein activity and the environment (Razzouk and Teixeira 2010). A database of the human metabolome has been created (Human Metabolome Database, HMDB) and may be compared to the bacterial metabolome in PICF. In summary, metabolomic techniques incorporate the influence of environmental factors along with host susceptibility (Razzouk and Teixeira 2010), therefore, metabolomics may fill the gap in knowledge of predicting peri-implant disease progression.

3. HYPOTHESIS AND AIM

Diagnosing peri-implant diseases using periodontal probing and radiographs may be inaccurate and only provides a historical record of past disease rather than current disease activity. Developing biomarker technologies may offer possibilities in diagnostic and prognostic application. As studies show the increasing prevalence of peri-implant diseases, increasing diagnostic and predictive accuracy may have a significant impact on dental care. Promising directions include the use of untargeted metabolomics in longitudinal trials to identify a unique set of biomarkers in PICF. Such a trial may also be able to determine the biomarkers' validity to diagnose peri-implantitis and predict which patients and which implants may be at risk of disease progression.

We *hypothesize* that the simple metabolites in peri-implant crevicular fluid (PICF) are diagnostic of peri-implantitis and are predictors of peri-implant disease progression.

We *aim* to define the unique set of metabolites in the PICF that establish a reliable method for early prediction of the deterioration of peri-implantitis.

4. MATERIAL AND METHODS

4.1 Study Design

Peri-implant crevicular fluid and salivary samples were collected from subjects with peri-implantitis as well as healthy implant controls at baseline and at six-month intervals for a total of 24 months. Clinical and radiographic examinations were also performed at baseline and each recall to obtain information regarding clinical indicators of peri-implant conditions. Peri-implant crevicular fluid and salivary samples were analyzed using nuclear magnetic resonance (NMR) spectroscopy. The study was approved by the Institutional Review Board at the University of Minnesota (Study number: 1511M79922). In this study, samples were collected from 71 implant subjects with a total of 151 implants.

4.2 Patient Selection, Inclusion and Exclusion Criteria

Diseased implants were diagnosed with PI if they showed at least one site around the affected implant with a pocket depth ≥ 6 mm and ≥ 3 mm of radiographic bone loss (RBL) measured from the implant-abutment interface (IAI) to the first bone-to-implant contact. Control healthy implants must exhibit healthy peri-implant tissues (PD ≤ 4 mm and RBL ≤ 2 mm from implant abutment interface). This definition intended to avoid overlapping between diseased and healthy sites due to measurement errors. Test and control subjects must be in good general health. Smoking habits were noted. Exclusion criteria include: 1) uncontrolled systemic disease, such as diabetes; 2) systemic antibiotic use within the past 3 months; 3) unable to provide consent; and 4) history of periodontal treatment or local antibiotic use in the past 12 months.

Subjects were selected among volunteers from patients presenting for treatment to the Graduate Periodontology Clinic at the University of Minnesota School of Dentistry from April 2015 to November 2018. Individuals who fulfilled the inclusion criteria were invited to participate in this study. The aim and the procedures of the study were discussed, and all patients signed a

consent and Health Insurance Portability and Accountability Act (HIPAA) form in accordance with the Declaration of Helsinki.

The first 3 recruited subject samples were eliminated due to sampling errors. The remaining subject pool (n=68) underwent further elimination of samples having errors such as pus or bleeding on the membrane, duplicates or missing NMR data output, 130 implant samples remained (n=61). 59 healthy implants (bone loss <2mm; PD ≤4mm; n=33) and 33 diseased implants (bone loss ≥3mm; PD ≥6mm; n=26) were statistically analyzed. The "other" group, (bone loss ≥ 2mm and <3mm; PD >4mm and < 6mm) contained 38 implants and was not included in the cross-sectional analysis as the implants did not meet the healthy nor diseased definitions yet were included in the longitudinal component to monitor possible future disease. Sampling, along with clinical and radiographic examinations were performed at 6, 12, 18 and 24 months. Only 47 patients (112 implants) were sampled longitudinally. Metabolomic profiles of untreated deteriorating implants that demonstrated progressive radiographic bone loss of > 1mm within a 6-month interval (Progressors: n=6) were compared to untreated diseased-non-progressing implants (n=8) and to healthy implants (n=26) which did not deteriorate throughout the trial duration.

4.3 Clinical Examination

Subjects seen for initial examination were assessed with a complete oral exam and clinical periodontal measurements. A Michigan-O probe with Williams markings color-coded probe 1-2-3-5-7-8-9-10 mm (CP-10 - Hu-Friedy) used with light to moderate pressure into the sulcus around implants to measure PD (free gingival margin to base of the pocket). BOP was noted with 3 categories: 1 absent; 2 pinpoint bleeding; 3 profuse bleeding and determined 30 seconds after probing of the site. Plaque was noted as absent or present by sliding the periodontal probe supragingivally across each one of the 6 sites per implant. All the implants that were PICF-sampled and clinically examined were assessed with intraoral non-standardized peri-apical

radiographs taken at 6, 12, 18 and 24 months to monitor bone levels around those implants over time.

4.4 Examiners and Calibration

Initial and periodic examinations and sample collections were carried out by calibrated examiners (i.e., periodontology residents). Radiographic bone loss measurements were carried out by Dr. Hatem Alassy. Calibration of residents was carried out annually.

4.5 Sample Procurement

Subjects were sampled at least 2 weeks but no later than 8 weeks after their initial periodontal examination, and before periodontal treatment is rendered. Each test individual was sampled at the deepest site of each implant affected by PI. Deep sites around test implants must have PD ≥ 6 mm. Each subject was sampled at 1 site of each implant to a maximum 4 implants per patient. Shallow sites around healthy implants in test and control individuals must be have PD ≤ 4 mm.

The sites were isolated and sampled individually. Each site was isolated with a cotton gauze and dried using a light air stream directed away from the sulcus and towards the coronal aspect of the implant's crown. Any supragingival plaque was removed using a curette, with care not to touch the free gingival margin or push supragingival plaque subgingivally. A 4 mm diameter 5-micron porous silver metal membrane was inserted into the pocket at each implant site with cotton pliers. The membrane was completely inserted into the sulcus/pocket until minimal resistance was felt. Using a timer, the membrane is left in place for 30 seconds. Any signs of contamination from blood or saliva was noted.

A saliva sample was also collected. Patients were asked to swallow excess saliva before placing the membrane on the dorsal side of the tongue for 30 seconds. All membranes were then placed in a pre-chilled Eppendorf tube containing a standardized buffer solution that had been kept on ice. The membranes were completely immersed in the buffer solution. Samples must

be labeled with (i) Subject ID; (ii) Implant site number (US standard); (iii) Location of sampling site around the implant; (iv) Health status of the site (Di {= deep implant site} or Si {= Shallow implant site}).

The Eppendorf tubes were vortexed to ensure full submersion of membranes into the buffer and centrifuged at 16,000 RPM's for 30 seconds. A micropipette was used to extract the supernatant while leaving the silver membrane behind. The supernatant was transferred into a new 2mL Eppendorf tube which is then stored at -80°C. The silver membranes were discarded within the original Eppendorf tube. Samples were removed from storage and thawed prior to being transferred from the Eppendorf tube to individual 1.7 x 103.5mm borosilicate tubes, SampleJet-cat#Z106462 – Bruker – Germany, via the aid of long gel-loading pipet tips, Sorenson-cat#13810, and refrigerated at ~5°C until NMR analyses were performed at the University of Minnesota NMR Center.

4.6 NMR analysis

Proton NMR analysis is performed at the Minnesota NMR center utilizing a Bruker Advance III 700-MHz spectrometer equipped with a 1.7mm cryogenic probe and a Sample Jet refrigerated sample changer. All 1,020 samples were analyzed in NMR over 9 batches of ~110 each from 2016-2020. A gradient-enhanced two-dimensional total correlation spectroscopy (2D 1H-1H TOCSY) pulse sequence with water suppression by excitation sculpting using 32 transients and 128 increments and a 7,000 Hz spectral width in each dimension was utilized.

4.6.1 Quantification of Metabolomic Profiles using NMR

2D NMR profiles were constructed by overlaying the 1D NMR sample spectra with that of the buffer control spectra. Opensource "rNMR" and "Chenomx" software were used to process the 2D NMR data, and 329 regions of interest (ROI) were manually defined around signals of cross-peaks which were based on Total Correlation Spectroscopy (TOCSY) data from public databases, Madison-Qingdao Metabolomics Consortium Database (MMCD)

and Human Metabolome Database (HMDB). ROIs were not defined on cross-peaks that appeared in the spectra for the buffer control samples. A review of the literature was performed to develop a list of metabolite identities associated with biochemical pathways suspected to play a role in periodontitis, since PI metabolomic data was lacking in the literature. This list was then used to identify and refine the manually defined ROIs resulting in 62 regions. This refinement allowed for a reduction of ROIs which encompassed overlapping signals from multiple metabolites. The Human Metabolome Database (HMDB) was used to label the metabolites. The maximum intensity for each ROI was then recorded to a spreadsheet and integrated with the corresponding clinical data forming a peak intensity table. Identification and assignment of specific metabolites was based on the two protons which most accurately matched and represented this metabolite. These proton resonances were then labeled as “metabolite.1” and “metabolite.2”, referring to the intensity of each proton measured by NMR. This trial identified 36 metabolites to be studied.

4.7 Statistical analysis

Demographic analysis was performed using chi square test, ANOVA and Student’s *t*-test. Metabolomic statistical analysis of data was performed using the web-based MetaboAnalyst 4.0 and 5.0 software suite (https://www.metaboanalyst.ca), (Chong, Wishart et al. 2019). The peak intensity table data was uploaded, filtered using interquartile range, normalized by median, log transformed and auto scaled. A principal component analysis (PCA) approach was used to test for the association between disease status (PD, RBL) and the top principal components (PCs). In metabolomics, PCA is used as a graphical representation for identifying patterns **(Figure 1A).** PCA is unbiased, since it ignores class labels while finding the variance in a dataset (Ozeki, Nozaki et al. 2016). Partial least squares discriminant analysis (PLS-DA) was then used to detect variable importance in projection (VIP) scores and estimate the predictive ability (Q2)

using 10-fold cross validation. The VIP score is “a weighted sum of squares of the PLS loadings that considers the amount of explained Y-variance of each component” (Chong, Wishart et al. 2019). This score identifies and ranks the foremost metabolites which appear to separate the groups. The higher the score the metabolite shows, the more important this metabolite is in the separation between the tested groups.

Variable selection using Least Absolute Shrinkage and Selection Operator (LASSO) was used to determine frequencies of the selected metabolite. LASSO is a regression analysis which enhances the accuracy of the model being tested. Ten-fold cross-validation was performed on LASSO to yield an unbiased estimate of prediction error so that the best number for markers could be selected. This analysis offers the best (and least) number of covariates (metabolites in this case) to be used as predictors between the groups. A pattern search using the “Pattern Hunter” feature in MetaboAnalyst was performed. This analysis helps in the identification of metabolites showing a particular pattern of change similar to one chosen metabolite. This pattern-matching method demonstrates the metabolites most likely and least likely to match the concentrations of another metabolite. The resulting image shows both positively correlated and negatively correlated compounds displayed in a bar graph.

Student’s *t*-test was performed for metabolite levels between specified groups to detect significant features using 0.05 as a cut-off P-value. We performed classical univariate receiver operating characteristics (ROC) curve analysis to calculate area under the curve (AUC) as well as their 95% confidence intervals, to compute optimal cutoffs for any given feature, as well as to generate performance tables for sensitivity, specificity, and confidence intervals at different cutoffs.

A good biomarker should have high sensitivity (a positive result when the disease is present) and high specificity (a negative result when the disease is not present). The sensitivity and specificity scores are usually shown as a percentage, for example, a sensitivity of 90% means that this biomarker test correctly identified 90% of samples (true positives) which actually had disease

but missed 10% of diseased samples. ROC curve analysis is used to describe the combination of both sensitivity and specificity of a certain test's performance in one chart. This diagram charts the true positive rate (y-axis {sensitivity}) against the false positive rate (x-axis {1-specificity}). If the specificity of a biomarker is 90% then this means that this marker correctly identified non-disease status 90% of the time and falsely identified 10% of the non-diseased samples as diseased. The x-axis of the ROC chart designates the specificity of the biomarker subtracted from 1. Therefore, a high specificity of 90% will be charted on the x-axis as 0.1 (1 – 0.9 = 0.1) indicating a low false positive rate. The best possible biomarker predictive value would be demonstrated as an optimal point on the upper left corner of the graph which indicates 100% sensitivity (1.0 true positive rate) and 100% specificity (0.0 false positive rate). The ROC AUC scores range between 0.5 – 1. The closer the biomarker's AUC analysis score is to 1.0, the more accurate this biomarker is. An AUC score value of 0.5 (along the diagonal line from lower left to upper right corners) indicates that there is no predictive value for this biomarker and that its assessment is not better than random. A value of 0.9 or more is considered excellent in accuracy while a value of 0.8 – 0.9 demonstrates good accuracy for this biomarker and a value of 0.7 – 0.8 is fair. However, a value of 0.6 – 0.7 is considered poor while a value between 0.5 – 0.6 is considered a failed marker (El Khouli, Macura et al. 2009).

We manually selected a combination of features to create a biomarker model that showed a higher AUC value than any single feature. Hierarchical clustering using the Euclidean distance measure and Ward algorithm was performed on the top 15 significant features ($p<0.05$) for visualization of the most contrasting patterns between the diseased and healthy groups.

R software is freely available, cross-platform compatible, and open source. Chenomx software fits 1D NMR data using reference spectra from a database. **Figure 1B** shows 1D data from one sample (black line), overlaid with the database spectra of lysine-related compounds in Chenomx. There is overlap between all compounds. Chenomx was used in generating

assignments, along with the HMBD and MMCD 2D NMR databases. The metabolites are present at very low levels in the

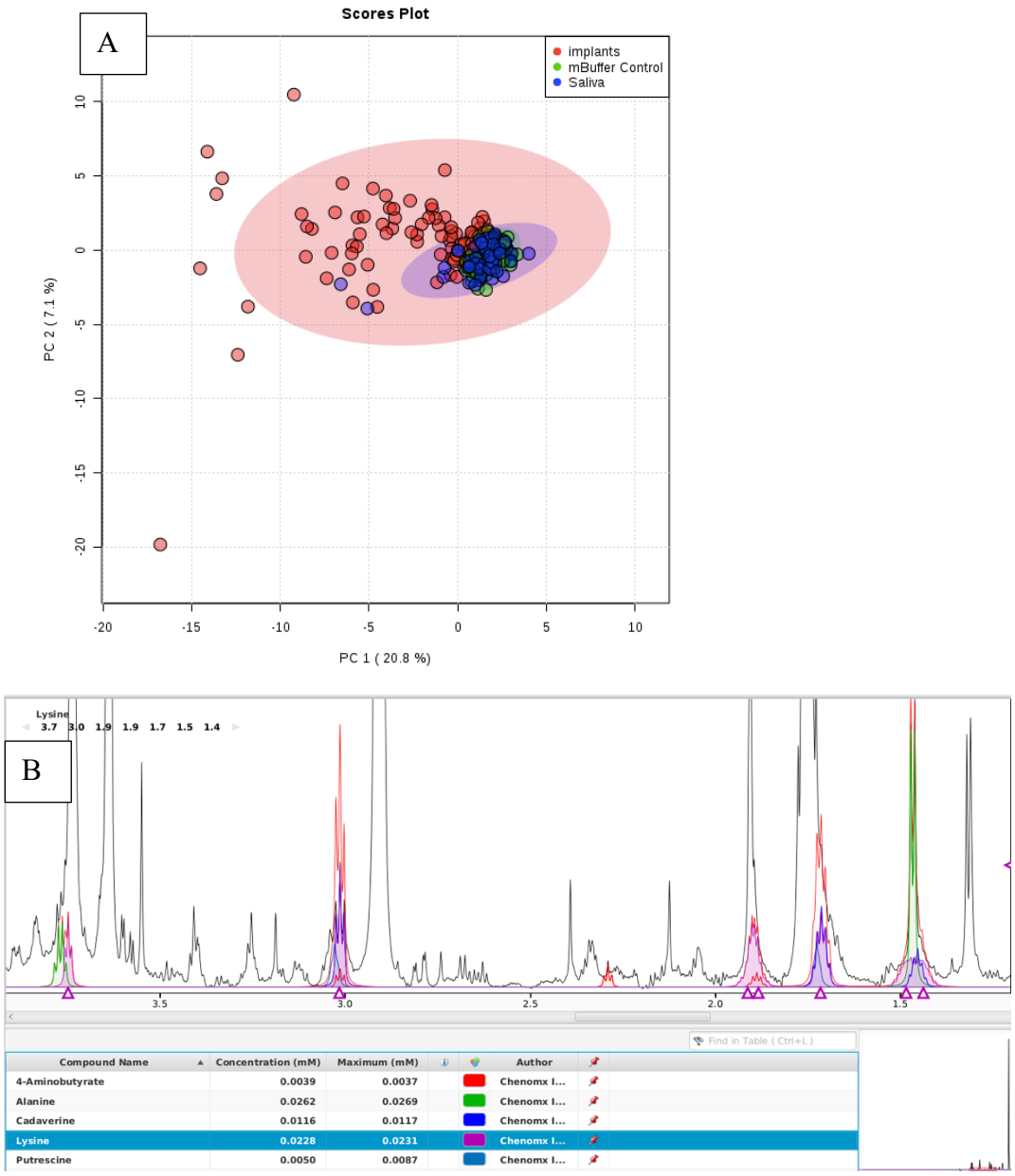

Figure 1. Metabolites around implants segregate from the metabolites in saliva and in buffer control samples. (A) Principal Component Analysis of metabolites comparing implants (red) vs saliva (blue) vs buffer controls (green). The quantity of metabolites in the PICF of all implants explain most of the variance between groups. **(B)** 1D data from one sample (black line), overlaid with the database spectra of lysine-related compounds in Chenomx software. There is overlap between compounds. The metabolites are present at very low levels which makes them difficult to fit, and the glycerol contamination (large signals around 3.8 in the spectrum) in a number of

samples drowns out the signals that would make it easier, for example, to differentiate alanine from lysine.

PICF samples which makes them difficult to fit, and the glycerol contamination (large signals around 3.8 in the spectrum in **Figure 1B**) in a number of samples drowns out the signals that would make it difficult, for example, to differentiate alanine from lysine.

After comparisons in a cross-sectional manner, the same analyses were performed for longitudinal comparisons. Longitudinal assessments were performed for sampling time-points of 6, 12, 18, and 24 months. For each time-point, clinical data was used to identify sites demonstrating a significant increase in RBL loss (at least 1mm). The metabolite profiles for each of these sites were compared to those of sites which are unchanged over the same duration. These unchanged sites are either healthy or diseased implants which did not progress (< 0.5mm RBL change). ANOVA-posthoc analysis was performed to compare 3 groups using MetaboAnalyst 5.0

5. RESULTS

5.1 Demographic data: Frequency distributions of variables

71 persons with 151 functioning implants participated. After elimination due to sampling errors, the remaining subject pool (n=68) included 47% males and 53% females having a mean age of 64.8 (SD= 9.8) **(Table 3).** Current smokers comprised 15% of the healthy implant group (n=4) and 12% of the PI group while past smokers comprised 31% of the healthy group (n=8) and 55% of the diseased group (n=18). 63 subjects had a periodontal diagnosis varying between slight to severe periodontitis. Age, gender and smoking status had no statistical significance between groups ($p>0.05$).

Table 3: Subject demographics.

Characteristics	Healthy Group (n=26)	Other Group (n=9)	Peri-implantitis Group (n=33)	Total Population (n=68)	p-value*
Age					
Mean (SD)	67.5 (10.9)	64.4 (7.0)	62.7 (9.2)	64.8 (9.8)	0.067
Gender					0.102
Males (%)	12 (46)	5 (56)	15 (45)	32 (47)	
Females (%)	14 (54)	4 (44)	18 (55)	36 (53)	
Smoking					0.275
Status	14 (54)	4 (44)	11 (33)	29 (43)	
Never (%)	8 (31)	5 (56)	18 (55)	31 (46)	
Previous (%)	4 (15)	0 (0)	4 (12)	8 (12)	
Current (%)					

Statistically significant p-value < 0.05.

5.2 CROSS-SECTIONAL COMPONENT

5.2.1 Peri-Implantitis was Associated with A Distinct PICF Metabolomic Profile

Metabolomics using NMR is used to discover biomarkers for diagnosis and prognosis of clinical conditions, and for mapping the metabolomic profile within a biological sample (Schirra and Ford 2017). The data is then analyzed to visualize patterns of metabolite intensities in correlation with a clinical condition (Ozeki, Nozaki et al. 2016). Unbiased methods are ideal for data exploration and analysis (Schirra and Ford 2017). Principal component scores can be plotted using PCA to identify clusters of correlated samples. Metabolite intensities were normalized to unit standard deviation before applying PCA to minimize the effect of confounders. A tight grouping among buffer control samples as well as saliva samples can be observed indicating a separation between controls, saliva and PICF metabolomic profiles (**Figure 1**). While a tight grouping among implants' healthy sites (green dots) compared to diseased sites (red dots) can be observed indicating that healthy sites share a similar metabolomic profile while diseased implants share a different metabolomic profile (**Figure 2**). The normalized spectra of metabolites demonstrated a significant separation between 59 healthy implants (RBL <2mm; PD ≤4mm; n=33) and 33 diseased implants (RBL ≥3mm; PD ≥6mm; n=26). Using PLS-DA analysis, eleven metabolites had a variable importance in the project (VIP) score >1.5 (**Figure 3**), which is a common minimum score to identify significance based on most other studies, (Al-Ani, Fitzpatrick et al. 2016, Kuboniwa, Sakanaka et al. 2016, Sakanaka, Kuboniwa et al. 2017, Strand, Tangen et al. 2019).

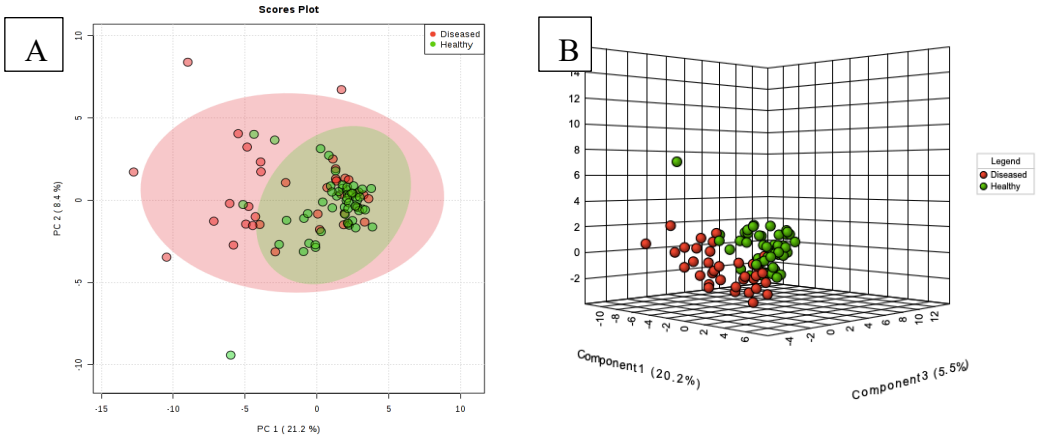

Figure 2: Diseased PICF metabolomic profiles are different from healthy samples. Score plots of Principal Component Analysis (PCA) of metabolites comparing diseased implants (red) and healthy implants (green) in **(A)** 2-dimensional and **(B)** 3-dimensional figures. The quantity of metabolites in the PICF of diseased sites explain most of the variance when compared to healthy implants. Tight grouping among healthy vs diseased implants can be observed indicating that healthy sites share a similar metabolomic profile while diseased implants share a different metabolomic profile.

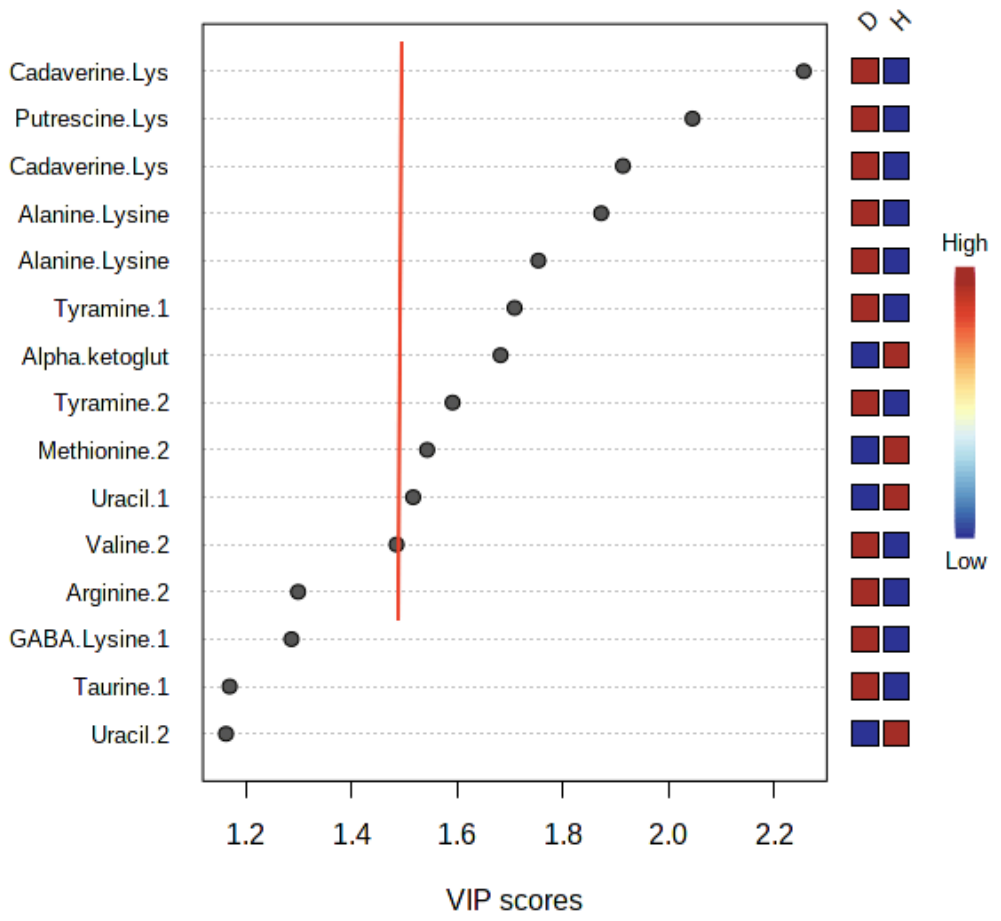

Figure 3. Cadaverine.Lysine is the top metabolite showing separation between diseased and healthy implant samples. Variable importance in projection (VIP) score ranks the top 15 metabolites (out of 35 total) showing separation between peri-implantitis vs healthy implant groups. Cadaverine/Lysine coherent proton resonances shows the highest relative concentration in diseased vs healthy implants. Metabolites having VIP scores over 1.5 (red line) are considered significant.

5.2.2. Specific PICF Metabolite Profiles Identified Peri-Implantitis Sites with Moderate Accuracy and Precision.

The area under the curve (AUC) in receiver operating characteristics (ROC) is a robust measure for comparing metabolite performance correlating with PI. ROC curve analysis is used to describe the combination of both sensitivity and specificity of a certain test's performance in one chart. The AUC scores range between 0.5 – 1. The closer the biomarker's AUC analysis score is to 1.0, the more accurate this biomarker is. An AUC value of 0.5 indicates that there is no predictive value for this biomarker. A value of 0.9 or more is considered excellent in accuracy while a value of 0.8 – 0.9 demonstrates good accuracy for this biomarker while a value of 0.7 – 0.8 is fair. However, a value of 0.6 – 0.7 is considered poor while a value between 0.5 – 0.6 is considered a failed predictive biomarker.

In univariate ROC curve analysis, Cadaverine/Lysine coherent proton resonance shows the highest validity in correlating with PI, AUC= 0.76 (95% CI 0.658-0.855, t-statistic= 4.39, p=0.00003) (**Figure 4**) compared to healthy implants while alpha-ketoglutarate was significantly associated with healthy implants, AUC= 0.706 (95% CI 0.593-0.819, t-statistic= -3.13, p= 0.002) (**Figure 5**). The PICF volume in healthy and in disease sites did not contribute to the difference among metabolites due to effective normalization of the data. This is corroborated by the assessment of Tyrosine where the ROC analysis as not correlated with diseased or healthy implants even though the volumes of PICF were presumably different in health versus disease sites (**Figure 6**).

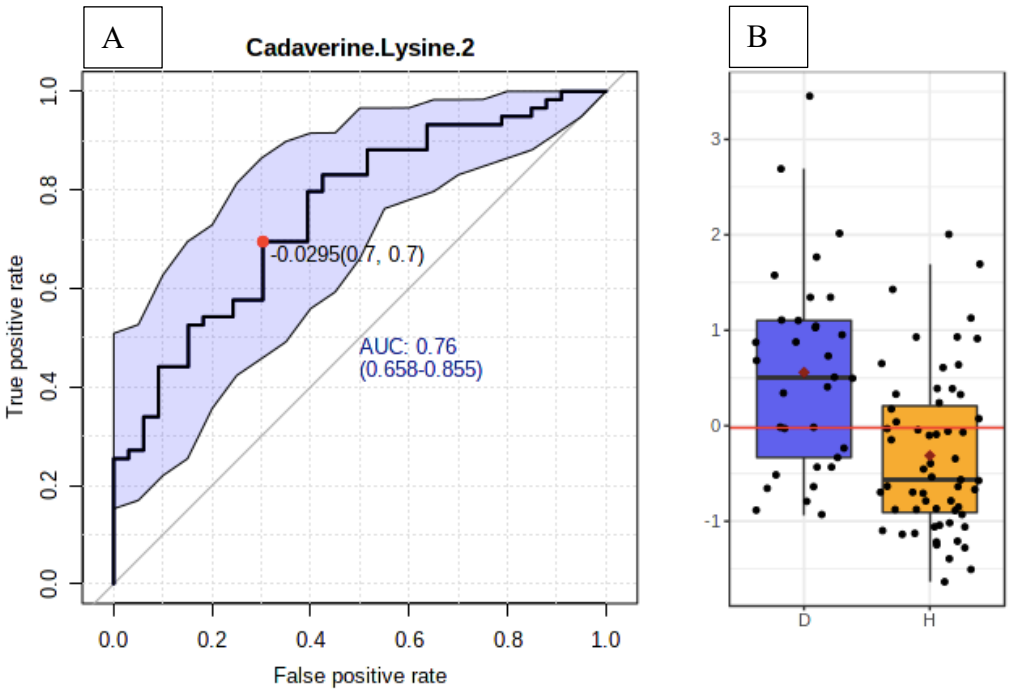

Figure 4: Cadaverine/Lysine shows high accuracy for the prediction of diseased implants. (A) ROC analysis curve for potential biomarkers demonstrate that Cadaverine/Lysine was significantly correlated with peri-implantitis AUC=0.76; 95% CI 0.658-0.855 (blue band). The solid red dot indicates the optimal cutoff with the associated sensitivity and specificity values. **(B)** Box-and whisker plot showing the distribution of abundance values between the two groups. The optimal cutoff is indicated as a horizontal red line.

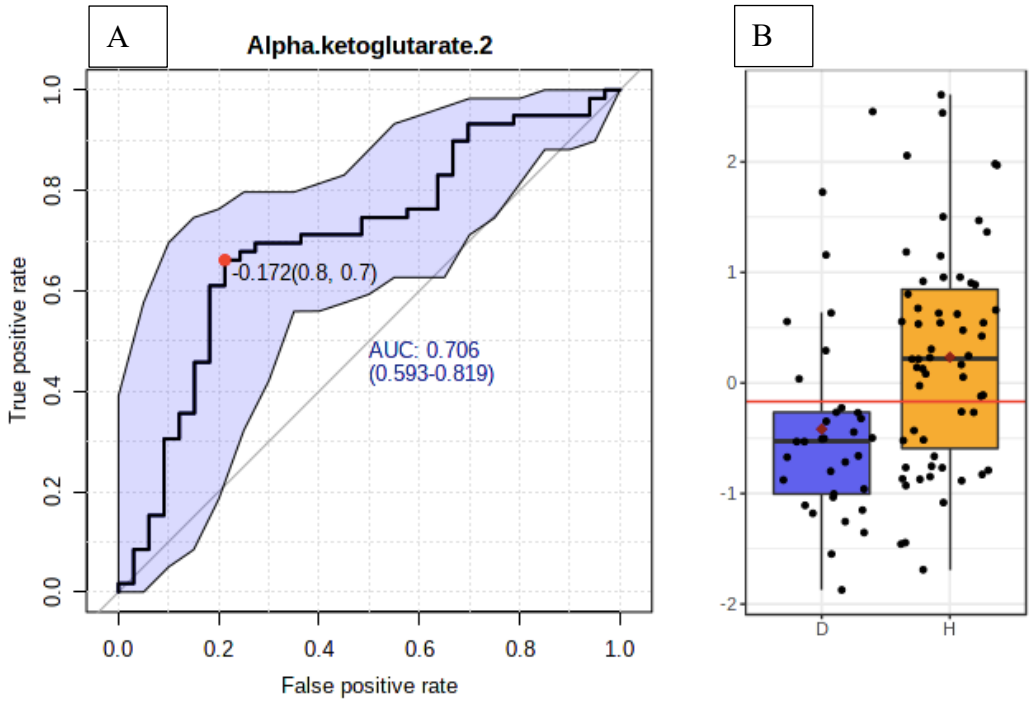

Figure 5: Alpha-Ketoglutarate shows high accuracy in the prediction of a healthy implant status. (A) ROC analysis curve for potential biomarkers demonstrate that Alpha-Ketoglutarate was significantly correlated with healthy implants AUC=0.706; 95% CI 0.593-0.819 (blue band) p= 0.002. **(B)** Box-and whisker plot showing a higher distribution of Alpha-ketoglutarate.2 abundance values in the healthy compared to the diseased group. The optimal cutoff is indicated as a horizontal line.

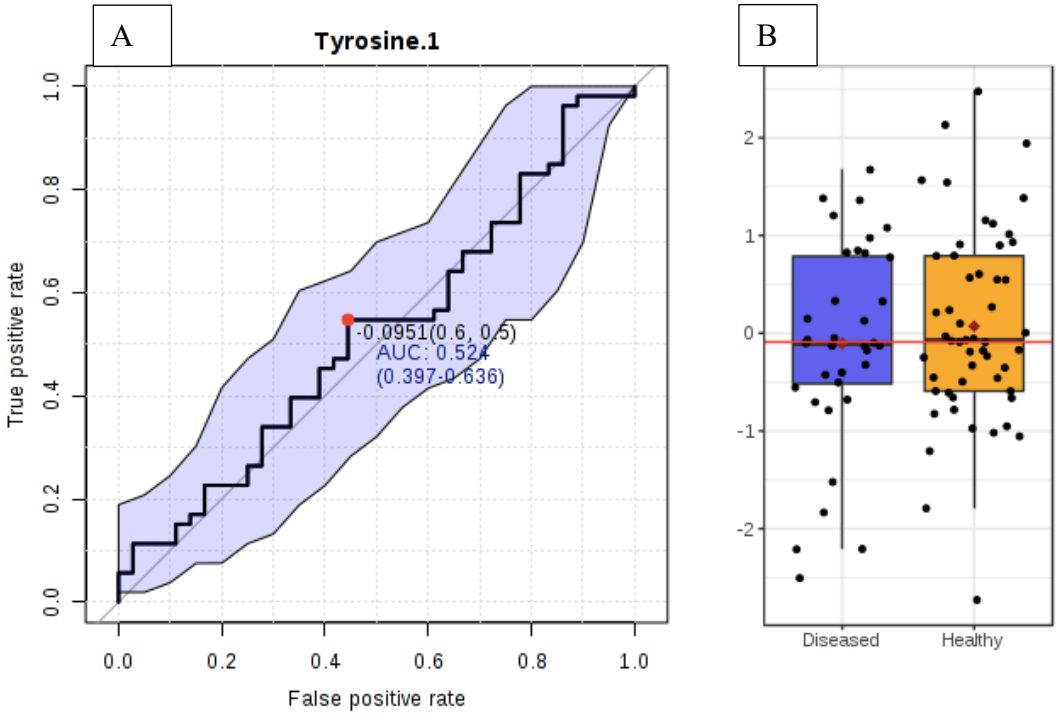

Figure 6: Tyrosine did not differentiate between healthy or diseased implant status. **(A)** ROC analysis for potential biomarkers showing Tyrosine was not correlated with diseased or healthy implants. **(B)** The right-hand image is the box-and-whisker plot showing the distribution of abundance values between the two groups. This validates normalization of data and shows that Tyrosine's relative concentrations were similar between healthy and diseased implants.

5.2.3. Combining Biomarkers Slightly Improved Predictive Accuracy

The 10-fold Cross-Validation was used to generate a logistic regression model and calculate the performance of combining 4 metabolite resonances. The ROC analysis demonstrated AUC=0.789 (95% CI 0.684-0.893, p<0.01). Combining several metabolites may offer a higher accuracy, compared to an individual metabolite, in discriminating between groups. The combination of cadaverine.lysine.2 with methionine.2, , offered high accuracy, in discriminating between healthy and diseased implants (AUC=0.81, 95% CI 0.645-0.915, p<0.01) (**Figure 7**), however this combination did not drastically improve on the accuracy found with Cadaverine.Lysine.2 resonance alone having AUC= 0.76 **(Table 4). Figure 8** illustrates the metabolites most likely and least likely to be present when Cadaverine/Lysine is present. This pattern search using Pearson correlation coefficient identifies metabolites showing either positive (pink) or negative (blue) correlation with Cadaverine/lysine. When Cadaverine/lysine is present in a sample then tyramine and putrescine/lysine were most likely to be found as well, while alpha-ketoglutarate is least likely to be present in the same sample.

Variable selection using Least Absolute Shrinkage and Selection Operator (LASSO) was used to determine frequencies of the selected metabolite resonance. LASSO is a regression analysis which enhances the accuracy of the model under study. Ten-fold cross-validation was performed on LASSO to yield an unbiased estimate of prediction error so that the best number for markers could be selected. LASSO modeling demonstrated the highest 3 frequencies were cadaverine.lysine.2, methionine.2 and putrescine.lysine (100%, 70% and 60% respectively). Therefore, cadaverine.lysine.2 would be an adequate single predictor and combining methionine.2 or putrescine.lysine may or may not add significant accuracy to the prediction model.

Since the PLS-DA model is prone to overfitting, we used cross-validation is to determine the optimal number of components needed to build the PLS-DA model. PLS-DA cross-validation demonstrated that a 1-component measure offered a significant accuracy of 0.727 (R^2=0.21, Q^2=0.12) **(Figure**

9). This indicates that only one component is adequate to accurately predict separation between the groups. While in multivariate analysis, the average predictive accuracy based on 100 cross validations was 0.661 (using Random Forest algorithm with 4 latent variables).

Table 4: Cadaverine.Lysine.2 and Alpha Ketoglutarate.2 show the highest positive and negative correlation with diseased implant status respectively. Student's *t*-test demonstrating t-statistic values of the 11 significant ($p<0.05$) features found in the cross-sectional component comparing peri-implantitis with healthy implants.

	t.stat	p.value	AUC
Cadaverine.Lysine.2	4.3933	3.0416E-05	0.75501
Putrescine.Lysine	3.9094	0.00017906	0.7093
Cadaverine.Lysine.1	3.6198	0.00048683	0.6831
Alanine.Lysine.1	3.5309	0.00065533	0.67386
Alanine.Lysine.2	3.2792	0.0014813	0.68105
Tyramine.1	3.1852	0.001988	0.66872
Alpha.ketoglutarate.2	-3.1304	0.0023538	0.70519
Tyramine.2	2.9447	0.0041139	0.64766
Methionine.2	-2.8475	0.0054587	0.65691
Uracil.1	-2.7943	0.0063554	0.67951
Valine.2	2.7316	0.0075855	0.6754

Positive correlations indicate that a higher concentration corresponds to increased disease presence while negative correlations indicate that a higher concentration corresponds to decreased disease presence. The AUC is a robust measure for comparing biomarkers' performance in correlation with peri-implantitis.

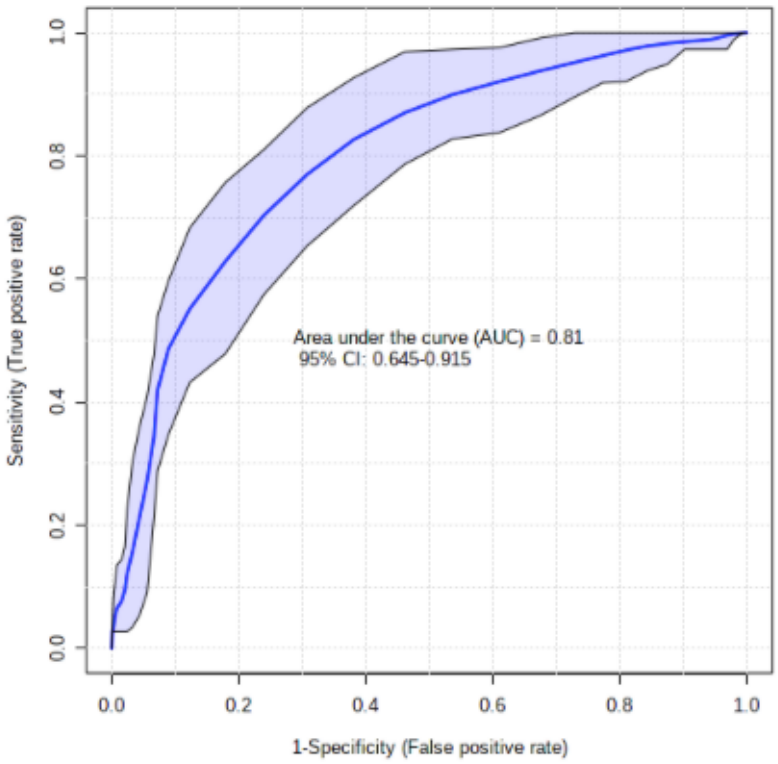

Figure 7: Combining two metabolites offered a slightly higher accuracy, compared to an individual metabolite, in discriminating between the groups. ROC analysis curve demonstrating the combination of cadaverine.lysine.2 and methionine.2 was able to accurately differentiate between diseased and healthy implant groups, AUC=0.81, 95% CI 0.645-0.915 (blue band), $p<0.01$.

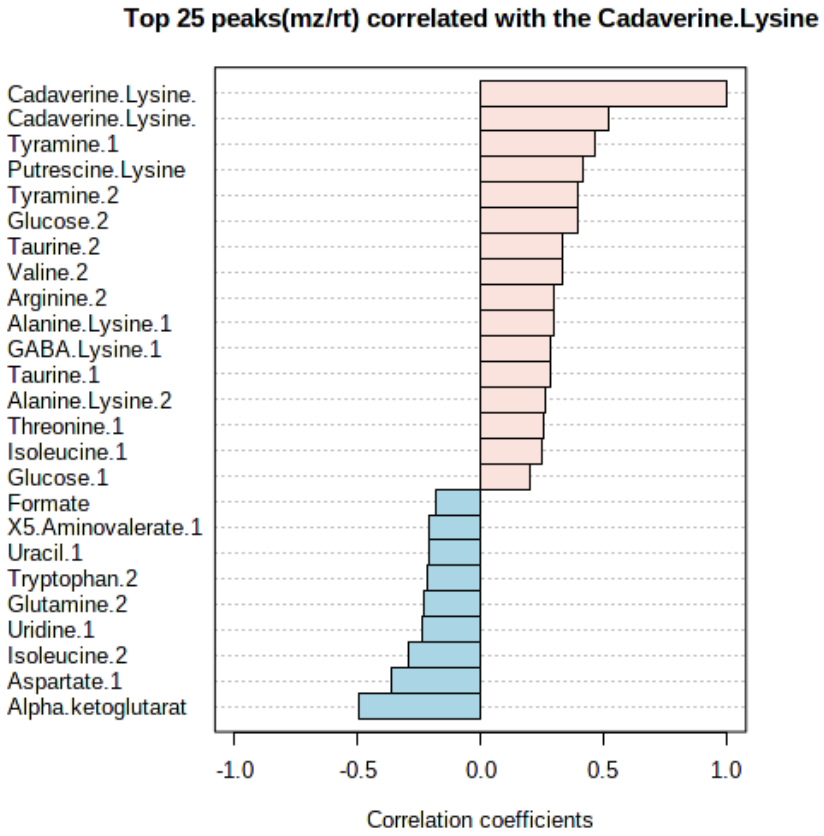

Figure 8: Metabolites most likely and least likely to be present when Cadaverine/Lysine is present. This Pattern search using Pearson correlation coefficient identifies metabolites showing either positive (pink) or negative (blue) correlation with Cadaverine/Lysine.

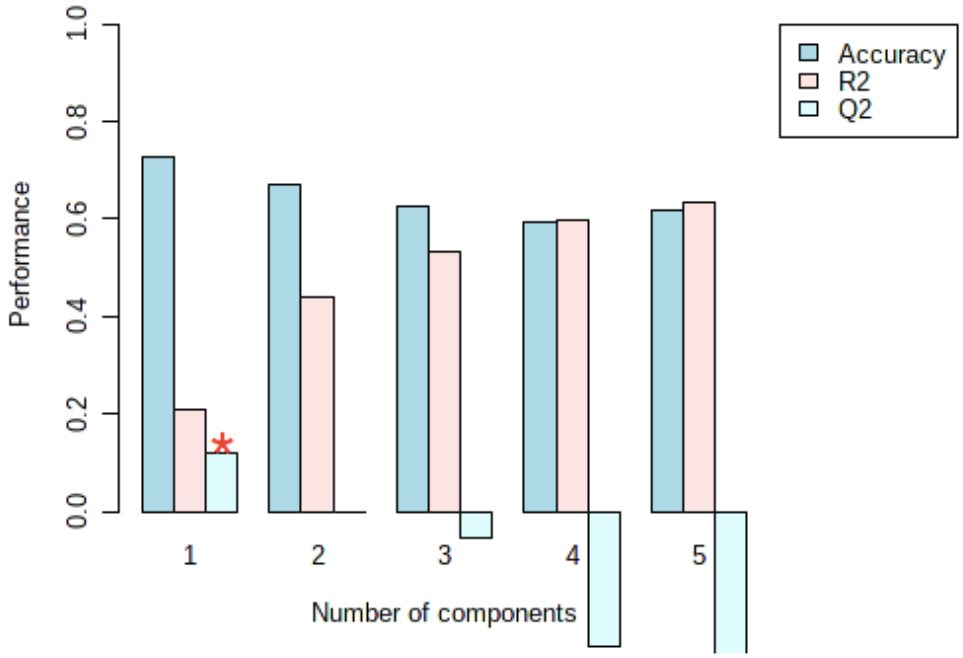

Figure 9: Cross validation for the PLS-DA correlation with peri-implantitis demonstrating that one metabolite accurately predicts diseased vs healthy implant status. Cross validation is performed to find the optimal number of components needed to create the PLS-DA model. The 3 common models are the sum of squares (R^2), cross-validation R^2 (Q^2) and Prediction Accuracy. The most common model is Q^2 which is an estimate of the predictive ability of the model and is calculated via cross-validation. Good predictions will have high Q^2. The red star indicates that only one component (metabolite) is adequate to accurately predict separation between the **diseased vs healthy implants**.

5.3 LONGITUDINAL COMPONENT

Out of the 71 subjects who entered the study, only 27 completed the 24-month samplings. While 24 subjects were only sampled once at baseline, 13 subjects were sampled twice, 6 subjects sampled 3 times, 14 sampled 4 times and 14 sampled 5 times. Some subjects missed their scheduled sampling visit and were subsequently sampled at the follow up visits. A total of 15 implants were explanted during the trial while 13 implants underwent surgical treatment.

A total of 9 subjects had 13 implants that progressed > 1mm of RBL loss over the course of the study. Seven samples were not analyzed either due to sampling errors or due to the subject missing a sampling visit. While only 6 untreated implants (in 4 subjects) were documented to have progressed > 1mm within a 6-month interval (**Table 5**). Only 4 implants were documented to have deteriorated within 12 months and 1 implant within 18 months. Within the deterioration periods, peri-implant pocket depths at sampling sites either remained the same (n=2), became deeper (n=4) or became shallower (n=3). Since peri-implant pocket depths were measured by multiple examiners, the radiographic data were chosen to document disease deterioration because they were measured by only one examiner. Radiographs of one example of a progressing implant within a 6-month interval is shown in **Figure 10**.

The healthy group included non-progressing healthy implants that remained healthy (< 0.5mm RBL change) at the following 6-month sampling (and throughout the trial period). A cut-off of 0.5mm was chosen for the healthy group to ensure health and stability of the implants in this group and to reduce the chance of including an implant which may be showing signs of deterioration. The diseased-non-progressing group included implants that remained stable (< 0.5mm RBL change) at the following 6-month sampling (and throughout the trial period) and that did not receive treatment either at the implant itself nor at the teeth/implants neighboring the implant that was measured. The surgically treated implants, 13 in total, were excluded from the analysis.

Table 5. Longitudinal component data table. Progressing implant samples at only the time point before their largest RBL loss (group A), untreated diseased-non-progressing and healthy implant samples from the time point before documented radiographic stability (group C and group B respectively).

	Subject ID	Sample	Group; A=progressor, C=diseased-non-progressor, B=healthy	Time Point	Implant	RBL mm	RBL loss (gain) mm at the following 6-month sample
1	UniMN005	19	A	1	4	3.25	1.15
2	UniMN043	253	A	1	23	8.85	2.4
3	UniMn018	343	A	3	21	3.25	2.08
4	UniMN005	400	A	4	3	2.07	1.53
5	UniMN064	704	A	1	3	0	5.2
6	UniMN064	705	A	1	4	2.08	4.94
7	UniMN019	79	C	1	3	3.30	0
8	UniMN026	109	C	1	30	3.8	(0.35)
9	UniMN036	177	C	1	12	5.15	0.31
10	UniMN043	254	C	1	26	5.07	(0.39)
11	UniMN053	420	C	1	20	4.49	(0.19)
12	UniMN059	567	C	1	25	3.12	0.12
13	UniMN070	999	C	3	3	5.33	(0.13)
14	UniMN070	1002	C	3	30	5.32	(0.52)
15	UniMN007	424	B	4	30	0	0
16	UniMN010	42	B	1	5	0	0
17	UniMN010	43	B	1	13	0	0
18	UniMN014	532	B	4	3	1.3	0.5
19	UniMN015	60	B	1	20	0	0
20	UniMN017	68	B	1	14	1.5	(0.2)
21	UniMN017	69	B	1	30	0	0
22	UniMN020	83	B	1	3	1.54	(0.505)
23	UniMN020	84	B	1	19	1.3	0.195
24	UniMN028	116	B	1	3	0.8	(0.8)
25	UniMN031	142	B	1	12	0	0
26	UniMN033	155	B	1	6	0.8	(0.8)
27	UniMN035	700	B	4	5	0	0
28	UniMN037	189	B	1	20	0	0
29	UniMN037	190	B	1	30	0.3	(0.3)

30	UniMN039	218	B	1	12	0	0
31	UniMN039	219	B	1	14	0	0
32	UniMN039	221	B	1	29	0	0
33	UniMN040	482	B	2	3	0.9	(0.375)
34	UniMN040	483	B	2	8	0.4	(0.4)
35	UniMN040	484	B	2	13	0.7	(0.7)
36	UniMN048	823	B	4	7	1.43	(0.13)
37	UniMN048	824	B	4	9	2.75	(0.99)
38	UniMN066	920	B	2	19	0	0
39	UniMN066	919	B	2	4	0	0
40	UniMN067	767	B	1	13	0	0

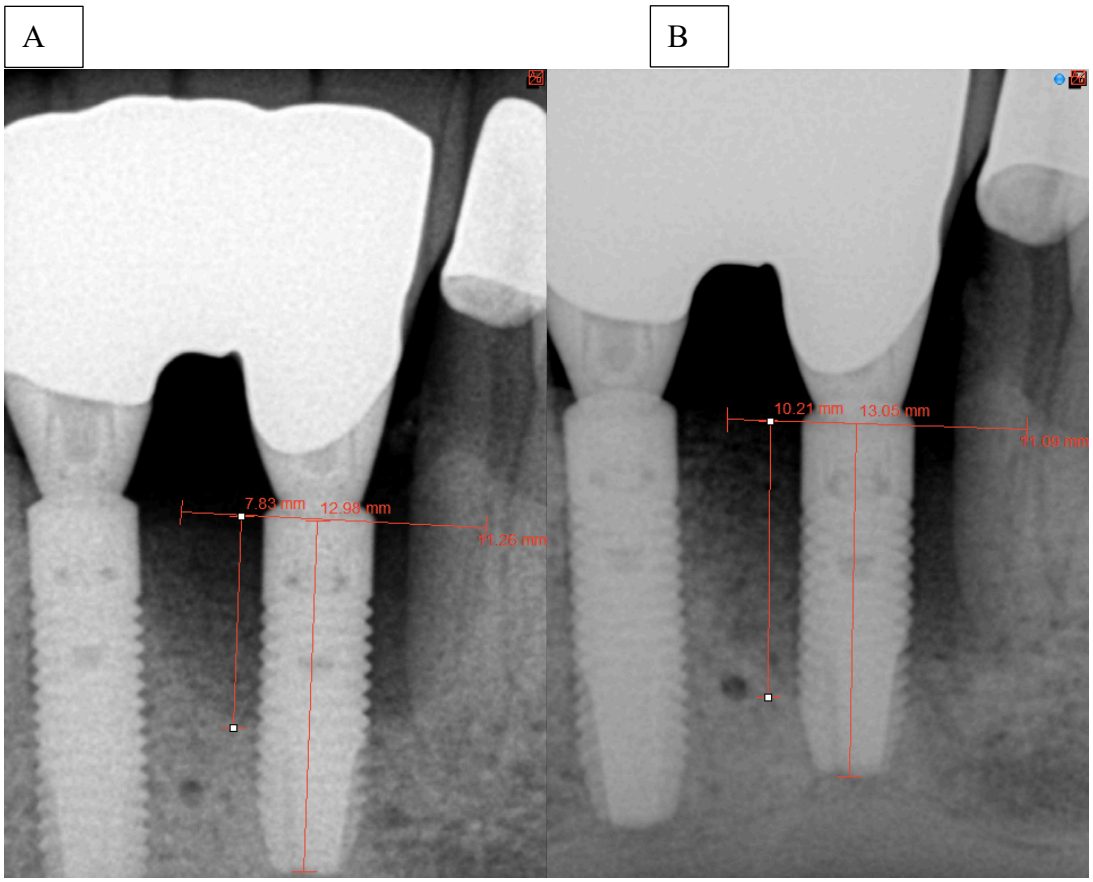

Figure 10. Non-standardized periapical radiographs of implant #23 showing > 2mm RBL within a 6-month period. (A) Bone loss of approximately 7mm is measured on this peri-apical radiograph. **(B)** Bone loss of approximately 10mm is measured on a second radiograph taken 6 months after the first radiograph. Since periapical radiographs were not standardized in this trial, foreshortening and elongation must be normalized. To obtain a true linear RBL value we used the calculation: (relative RBL) X (actual implant length / relative implant length). Since patient records indicated this implant to be 12mm then the true linear RBL in **(A)** is 7.83 X 12/12.98 = 7.24mm while the true linear RBL in **(B)** is 10.21 X 12/13.05 = 9.39mm.

5.3.1 Each of the three groups demonstrated a distinct metabolomic profile

The progressors group (group A; n=6; containing samples from only the time point of before their largest RBL loss) were compared to healthy implants (group B; n=26) and to diseased-non-progressors (group C; n=8). The metabolites levels of the three groups differ significantly as demonstrated by the PLSDA plot (**Figure 11**). The VIP score plot (**Figure 12**) shows the top 15 metabolites, 7 of which have a VIP score above 1.5 demonstrating a high level of significance. The VIP score is a mathematical algorithm which determines and ranks the foremost metabolites which separate between the groups. This is “a weighted sum of squares of the PLS loadings that considers the amount of explained Y-variance of each component” (Chong, Wishart et al. 2019). The higher the score the metabolite shows, the more important this metabolite is in the separation between the tested groups. The VIP score ranks the metabolites with the highest concentration difference between the two groups.

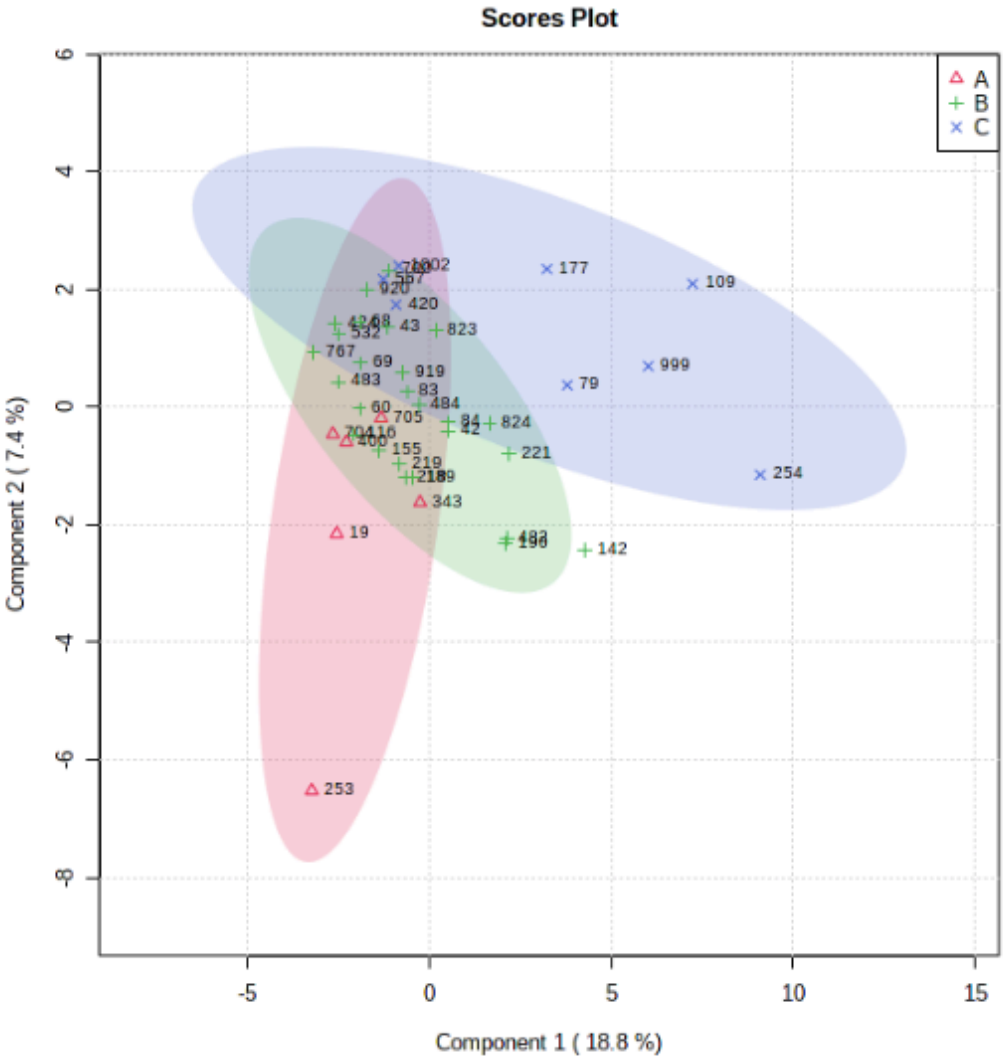

Figure 11. PLSDA plot demonstrating metabolite profile separation between the 3 groups. Progressing implant samples from all sampling time points (group A in red) showed separation from healthy implant samples (group B in green) and compared to diseased-non-progressing implants (group C in blue).

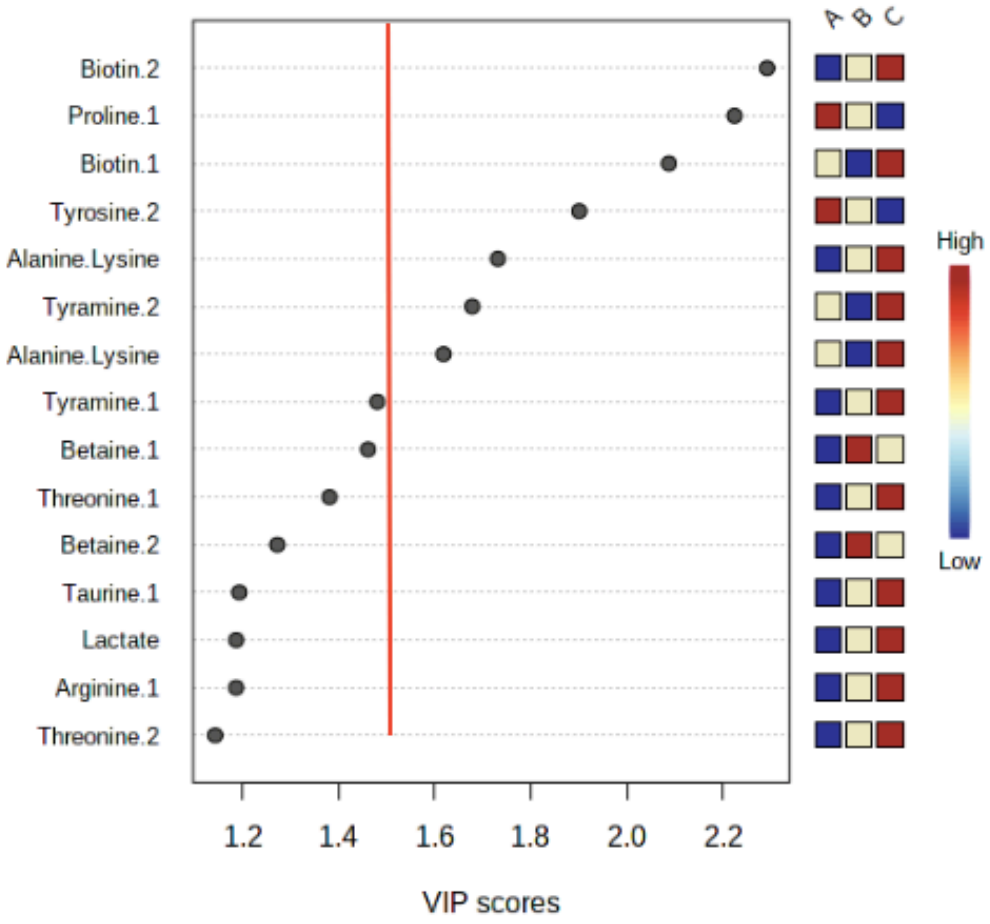

Figure 12. VIP scores showing the top 15 metabolites 7 of which have a VIP score above 1.5 (red line) demonstrating a high level of significance. Progressors (group A) show high scores in proline and tyrosine while the healthy implants (group B) show a high level of betaine and the diseased-non-progressing implants (group C) demonstrate high scores in biotin, alanine-lysine and tyramine.

A one-way ANOVA-posthoc comparison of metabolite profiles between the 3 groups was performed and identified statistically significant separation in the molecular signatures of biotin, propionate and valine, (**Table 6** and **Figure 13**). Biotin was significantly associated with diseased-non-progressors compared to both progressors and healthy implants ($p < 0.000$; AUC= 0.889; VIP> 2.0). Propionate was significantly higher in diseased-non-progressors compared to healthy implants ($p = 0.001$; AUC= 0.87). While Valine was significantly correlated in both progressors and diseased-non-progressors compared to the healthy group ($p = 0.002$; AUC= 0.841).

Table 6. Four metabolite resonances significantly separate between the 3 groups in the longitudinal component. One-way anova-post-hoc analysis. Groups A=progressors, B=healthy, C=diseased-non-progressors. Biotin1 and biotin2 were significantly higher in diseased-non-progressors compared to both progressors and healthy implants (p< 0.000). Propionate was significantly higher in diseased-non-progressors compared to healthy (p= 0.001). While Valine was significantly higher in both progressors and diseased-non-progressors compared to the healthy group (p= 0.002).

	f.value	p.value	-log10(p)	FDR	Fisher's LSD
Biotin.1	12.767	6.0758E-05	4.2164	0.003524	C - A; C - B
Biotin.2	11.159	0.00016131	3.7923	0.0046781	C - A; C - B
Propionate	7.6524	0.0016547	2.7813	0.031991	C - B
Valine.2	6.8959	0.0028481	2.5454	0.041298	A - B; C - B

A

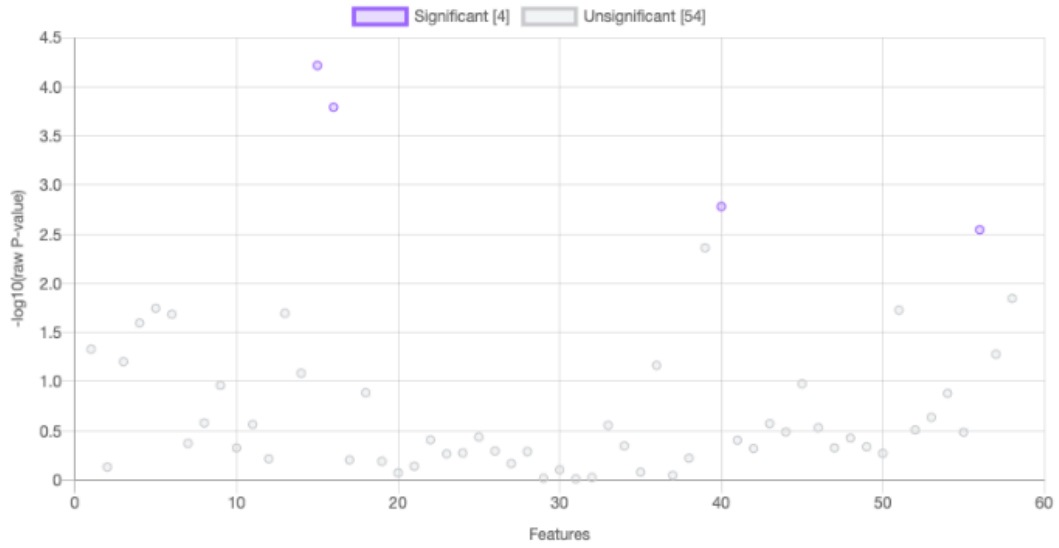

Legend in next page

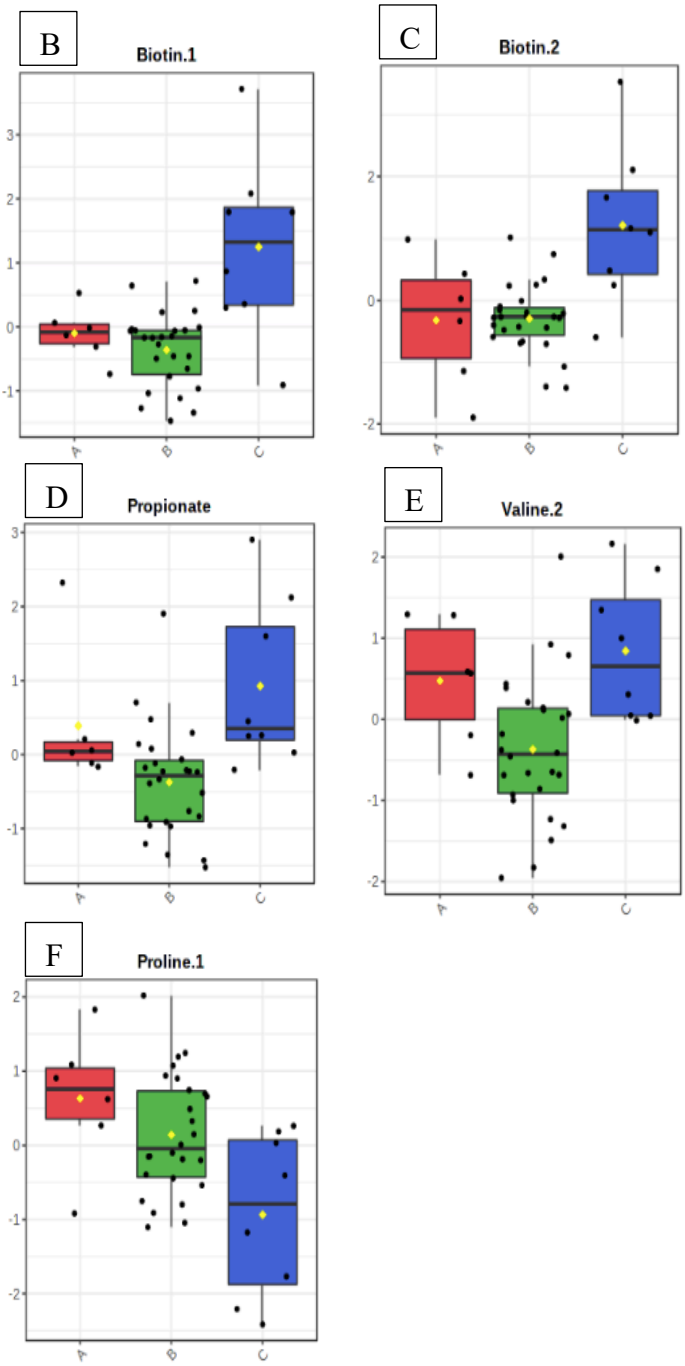

Figure 13. Significant metabolites separate between progressors, diseased-non-progressors and healthy implants. (A) The purple dots on the plot are the 4 metabolites (biotin1, biotin2, propionate and valine2) showing statistical significance ($p < 0.05$) between progressors, diseased-non-progressors and healthy implants. **(B-F)** Box and whisker plots shows metabolite separation between the groups. **(B-C)** Biotin1 and biotin2 were

significantly higher in diseased-non-progressors compared to both progressors and healthy implants ($p < 0.000$). **(D)** Propionate was significantly higher in diseased-non-progressors compared to healthy ($p = 0.001$). **(E)** Valine was significantly higher in both progressors and diseased-non-progressors compared to the healthy group ($p = 0.002$). **(F)** Proline1 did not show statistical significance in the anova analysis, however, demonstrated higher means progressors followed by healthy followed by diseased-non-progressors.

5.3.2 Biotin, propionate, valine and proline significantly separated diseased-non-progressors from healthy implants

PLSDA and VIP plots and Student's *t*-tests were performed to further analyze the differences between groups. When the diseased-non-progressors (group C) were compared to the healthy group (group B); proline1 was found to be correlated with the healthy group ($p= 0.004$; AUC= 0.755; VIP> 1.8) (**Table 7**). While biotin, propionate and valine significantly correlated with the diseased-non-progressing implants ($p< 0.002$). Furthermore, such correlation for biotin and propionate had VIP scores > 2.0 and a Q^2 predictive value of 0.2 indicating high accuracy (**Figure 14**). The ROC analyses plot demonstrating high validity (AUC: 0.755-0.889) in separation between 5 metabolites in healthy implant sites compared to diseased-non-progressing implant sites (Figure 15). Box and whisker plots of the statistically significant ($p< 0.05$) metabolites demonstrating that biotin1, biotin2, propionate2 and valine2 are correlated with diseased-non-progressors while proline1 was higher in healthy implants.

Table 7. Five metabolite resonances separate between Diseased-non-progressors group vs the healthy group in this t-test. A positive t-statistic indicates a correlation with healthy while a negative t-statistic indicates correlation with diseased-non-progressors. When the diseased-non-progressors were compared to the healthy group; proline1 was found to be correlated with the healthy group (p= 0.004).

	t.stat	p.value	-log10(p)	FDR
Biotin.2	-4.908	2.5957E-05	4.5858	0.0011591
Biotin.1	-4.7591	3.9968E-05	4.3983	0.0011591
Propionate	-3.7989	0.00061395	3.2119	0.01187
Valine.2	-3.3584	0.002037	2.691	0.029537
Proline.1	3.0843	0.0041837	2.3784	0.04853

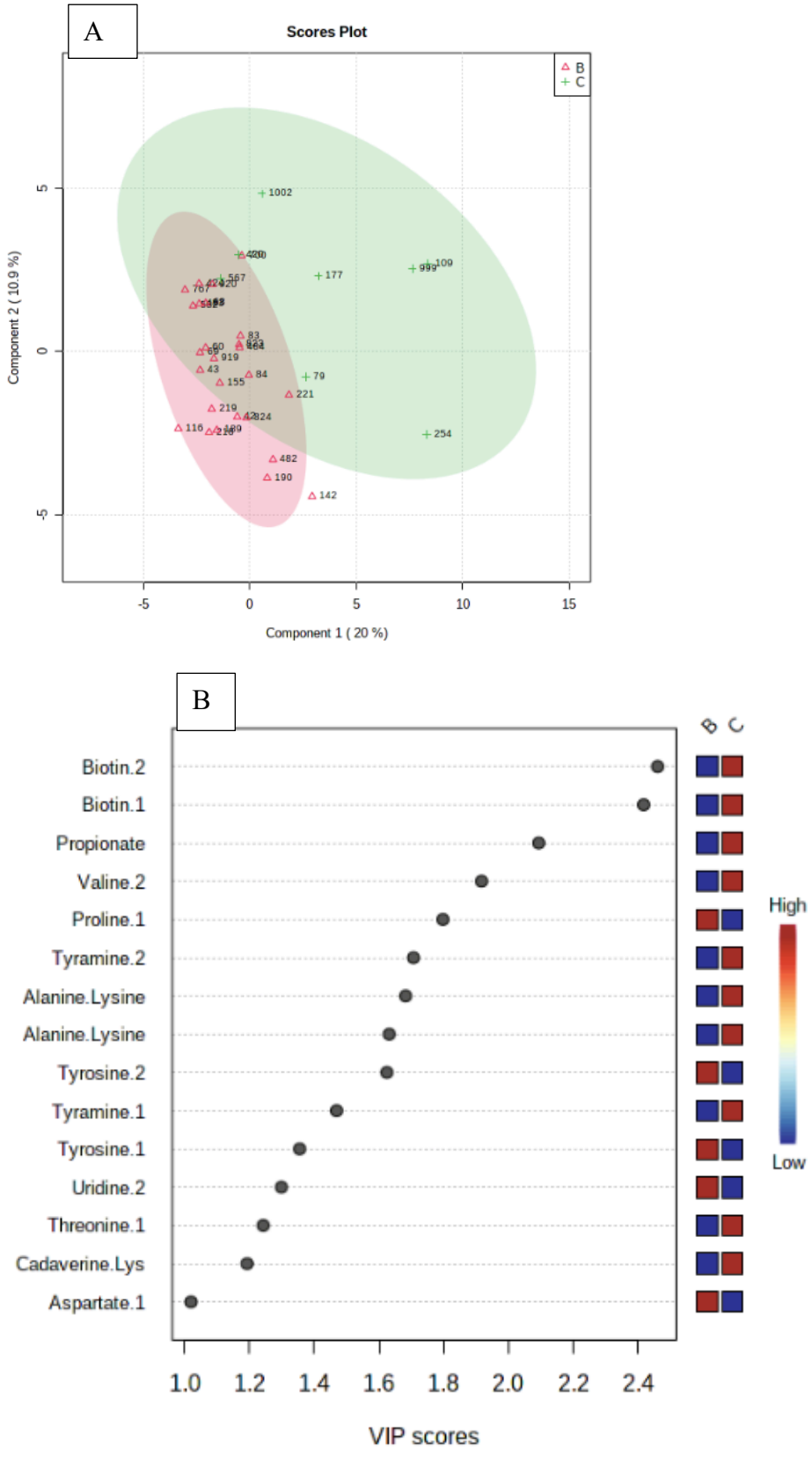

Legend in next page

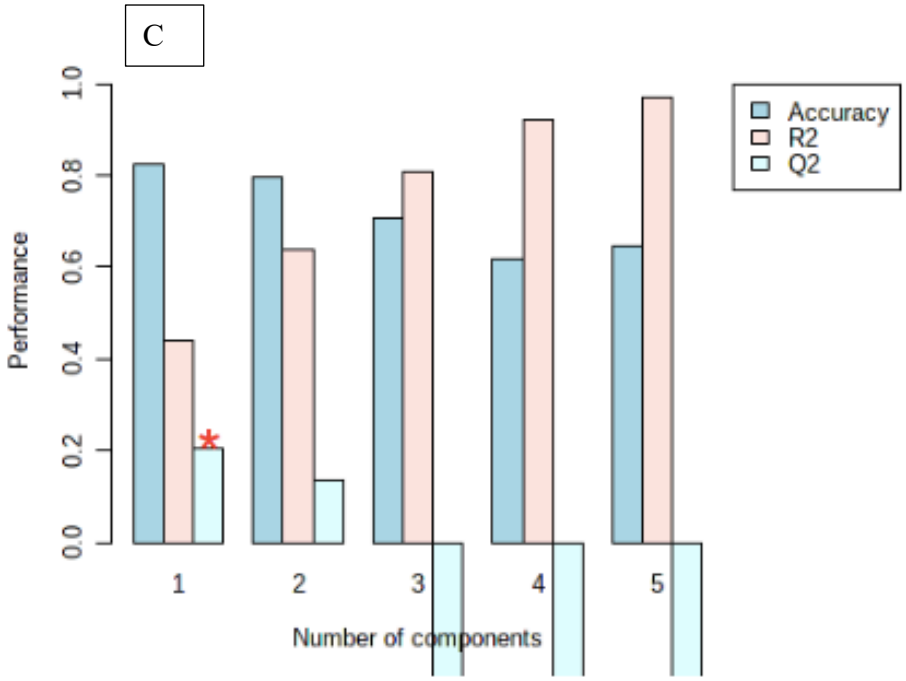

Figure 14. Significant metabolites show separation between healthy and diseased-non-progressor groups. (A) PLS-DA plot demonstrating separation between metabolites in healthy (B, red) implant sites compared to diseased-non-progressors (C, green) implant sites. **(B)** VIP scores showing the top 15 metabolites 9 of which have a VIP score above 1.5 demonstrating a level of significance. **(C)** Cross validation chart demonstrating a Q^2 predictive value of 0.2 indicating high accuracy.

5.3.3 Progressing implants demonstrated a distinct metabolomic profile prior to bone loss

The progressors' samples at only the time point of before their largest RBL loss were identified (group A) and compared with diseased-non-progressing implants (group C) that showed no deterioration (< 0.5mm change) in RBL in their following sampling visits. Since the sample size of the progressing implants was small (n=6), statistical significance was not achieved when studying these implants immediately prior their deterioration measured via radiographic bone loss. A PLS-DA plot comparing progressors (group A) with diseased-non-progressors (group C) demonstrated a tight grouping of metabolites separating the groups (**Figure 16**). High accuracy in the ROC analysis was demonstrated in figure 16b. Proline and 1-3-diaminopropane were higher in the progressors with AUC= 0.917 and 0.854 respectively. While Glucose was correlated with the diseased-non-progressors (AUC= 0.896).

Another PLS-DA plot comparing progressors (group A) with healthy implants (group B) demonstrated a tight grouping of metabolites separating the groups (**Figure 17**), yet statistical significance was not reached. However, high accuracy in the ROC analysis, figure 17, was demonstrated by the correlation of 1-3-diaminopropane with the progressors (AUC= 0.84) while betaine and arginine were correlated with healthy implants (AUC= 0.827 and 0.801 respectively).

In summary, the cross-sectional component of this study demonstrated that simple metabolites in PICF are diagnostic of peri-implantitis since specific metabolites differentiated between the healthy and diseased groups with moderate accuracy. These simple metabolites were namely cadaverine.lysine and alpha ketoglutarate. The longitudinal component of this trial mapped a specific metabolomic profile able to identify implants in health versus progressive disease versus a non-progressing disease status. Therefore, PICF metabolites reliably predicted the deterioration of peri-implantitis.

A

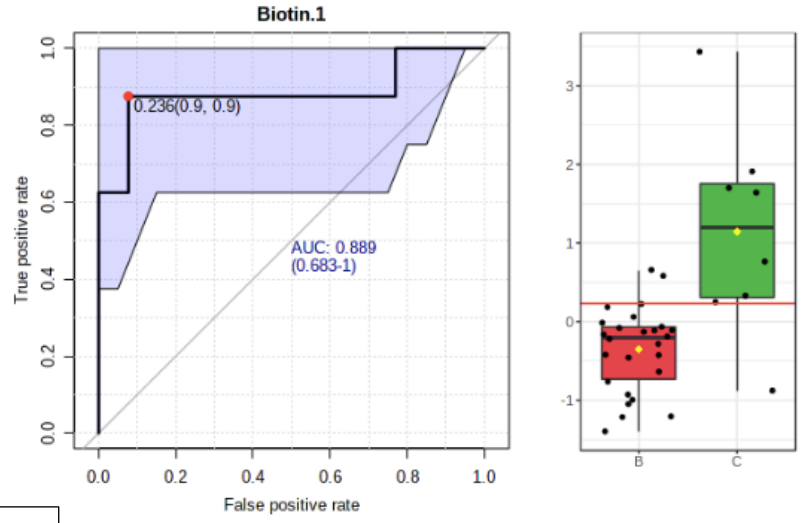
Biotin.1
0.236(0.9, 0.9)
AUC: 0.889
(0.683-1)
True positive rate
False positive rate
0.0
0.2
0.4
0.6
0.8
1.0
B
C

B

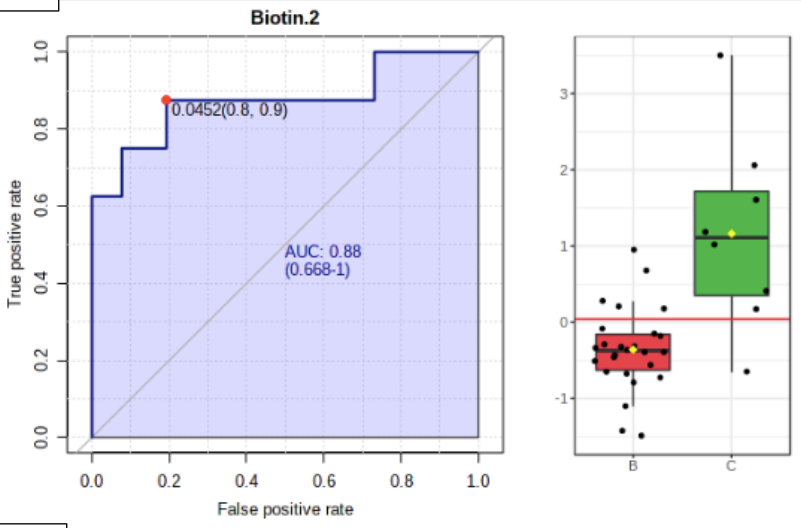
Biotin.2
0.0452(0.8, 0.9)
AUC: 0.88
(0.668-1)
True positive rate
False positive rate
0.0
0.2
0.4
0.6
0.8
1.0
B
C

C

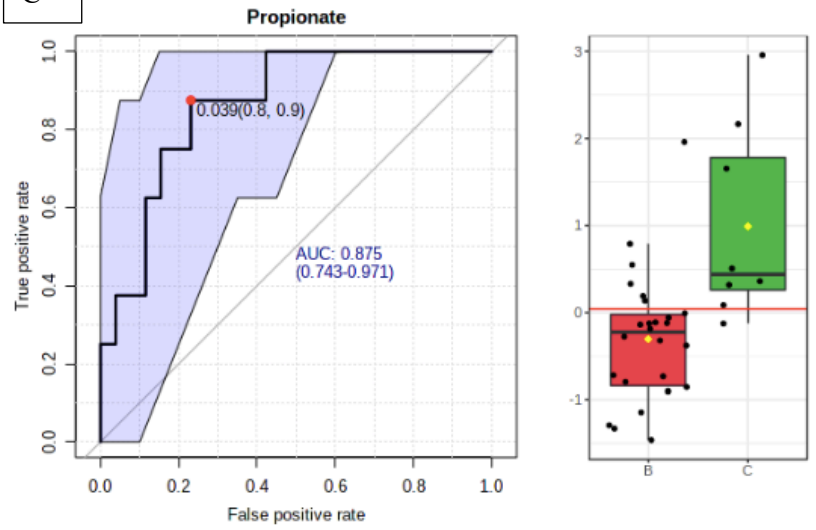
Propionate
0.039(0.8, 0.9)
AUC: 0.875
(0.743-0.971)
True positive rate
False positive rate
0.0
0.2
0.4
0.6
0.8
1.0
B
C

Legend in next page

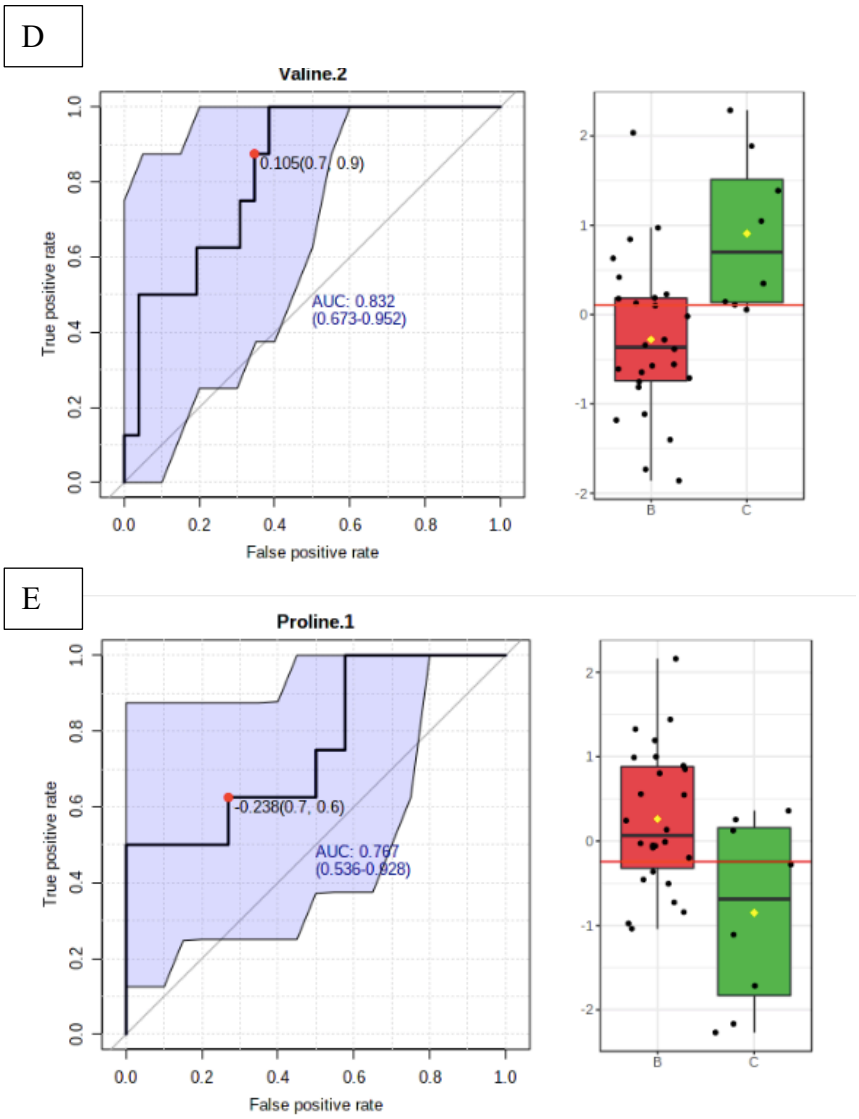

Figure 15. ROC analyses and Box and whisker plots demonstrating good accuracy (AUC: 0.755-0.889) in separation between 5 metabolites in healthy implant sites compared to diseased-non-progressing implant sites. The blue band represents the 95% confidence interval while the solid red dot indicates the optimal cutoff with the associated sensitivity and specificity values. **(A-D)** Box and whisker plots of the statistically significant ($p < 0.05$) metabolites demonstrating that biotin1, biotin2, propionate2 and valine2 are correlated with diseased-non-progressors while, **(E)** proline1 was higher in healthy implants.

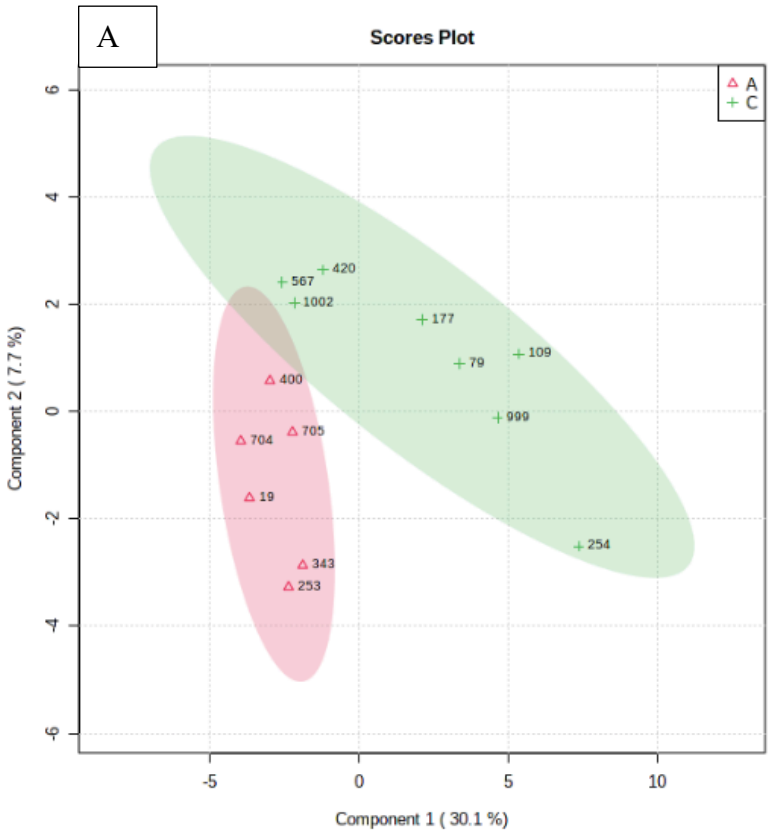

Legend in next page

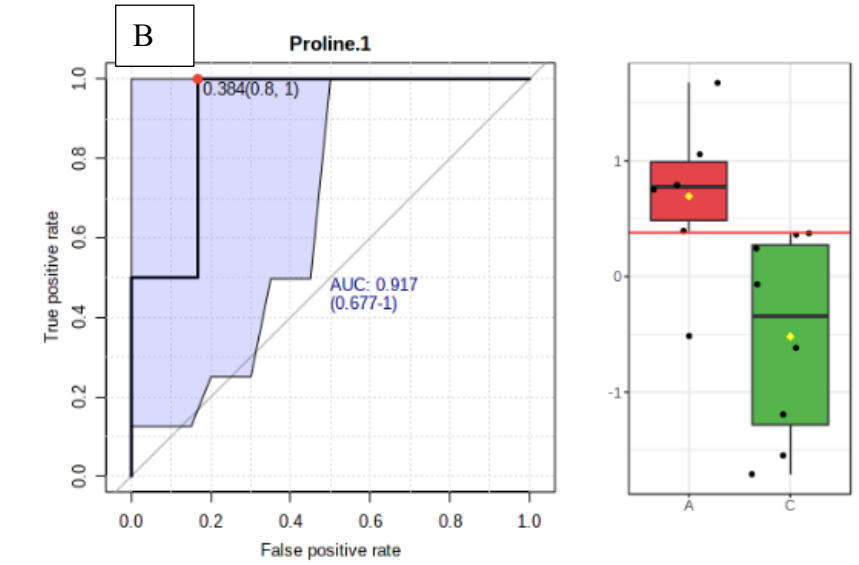
B
Proline.1
0.384(0.8, 1)
AUC: 0.917
(0.677-1)
True positive rate
False positive rate
0.0
0.2
0.4
0.6
0.8
1.0
1
0
-1
A
C

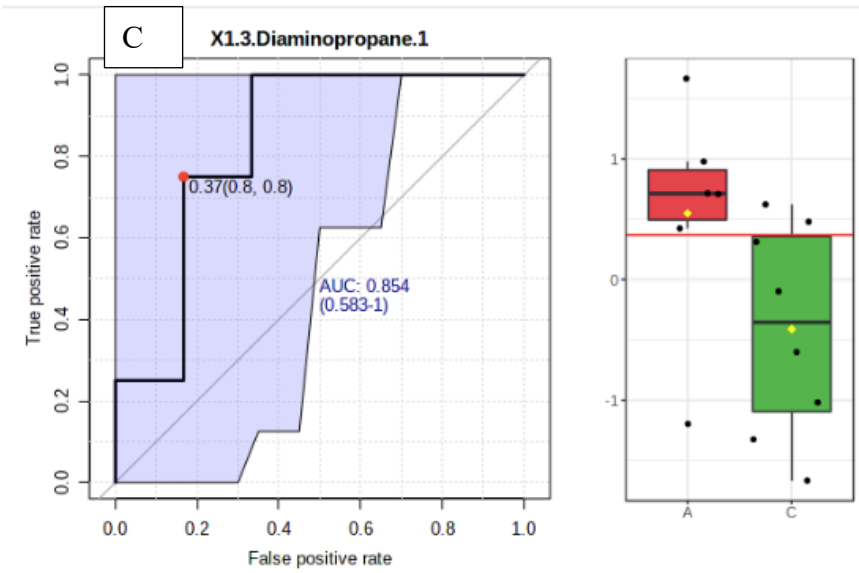
C
X1.3.Diaminopropane.1
0.37(0.8, 0.8)
AUC: 0.854
(0.583-1)
True positive rate
False positive rate
0.0
0.2
0.4
0.6
0.8
1.0
1
0
-1
A
C

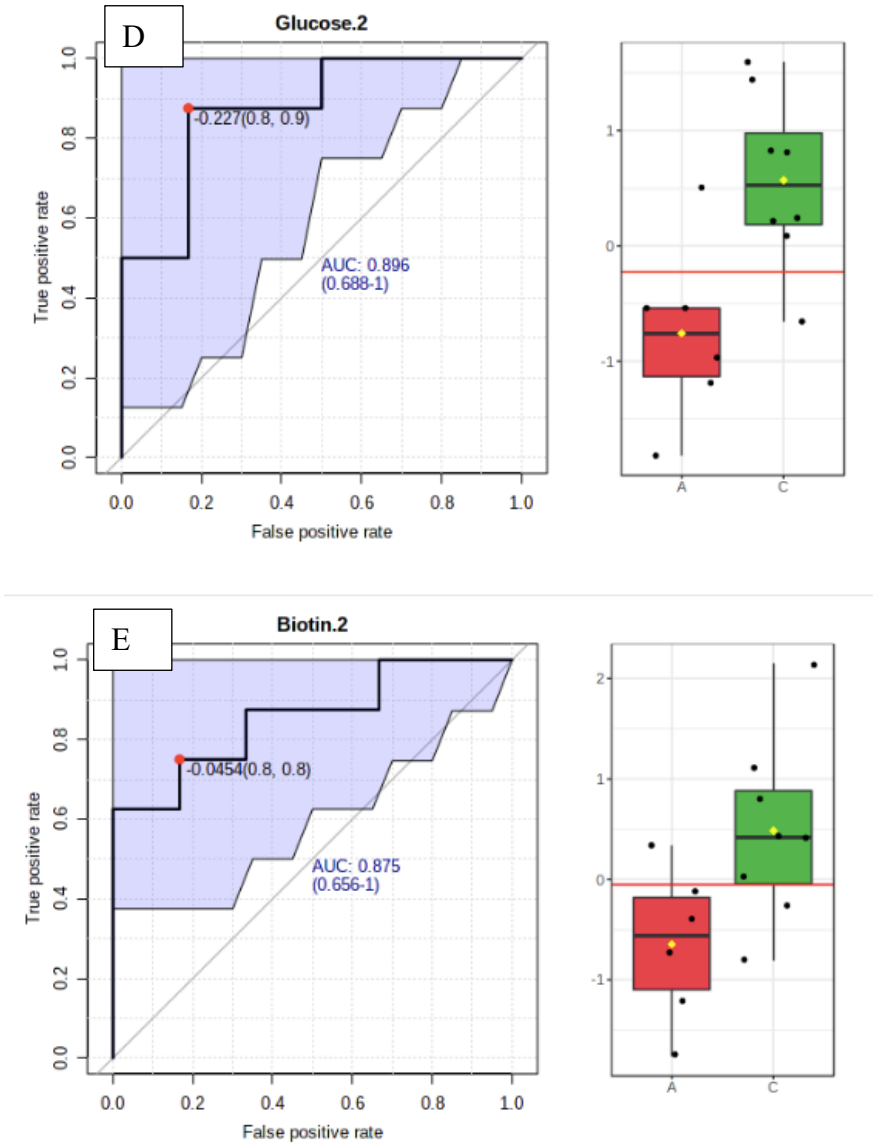

Figure 16. Significant metabolites showing separation between progressors and diseased-non-progressor groups. (A) PLS-DA plot comparing progressors (group A, red) with diseased-non-progressors (group C, green) demonstrating a tight grouping of metabolites separating the groups, yet statistical significance was not reached. **(B-E)** High accuracy in the ROC analysis was demonstrated. Proline and 1-3-diaminopropane were higher in the progressors with AUC= 0.917 and 0.854 respectively. While glucose.2 and biotin.2 were correlated with the diseased-non-progressors (AUC= 0.896 and 0.875 respectively). The blue band represents the 95% confidence interval while the solid red dot indicates the optimal cutoff with the associated sensitivity and specificity values.

A

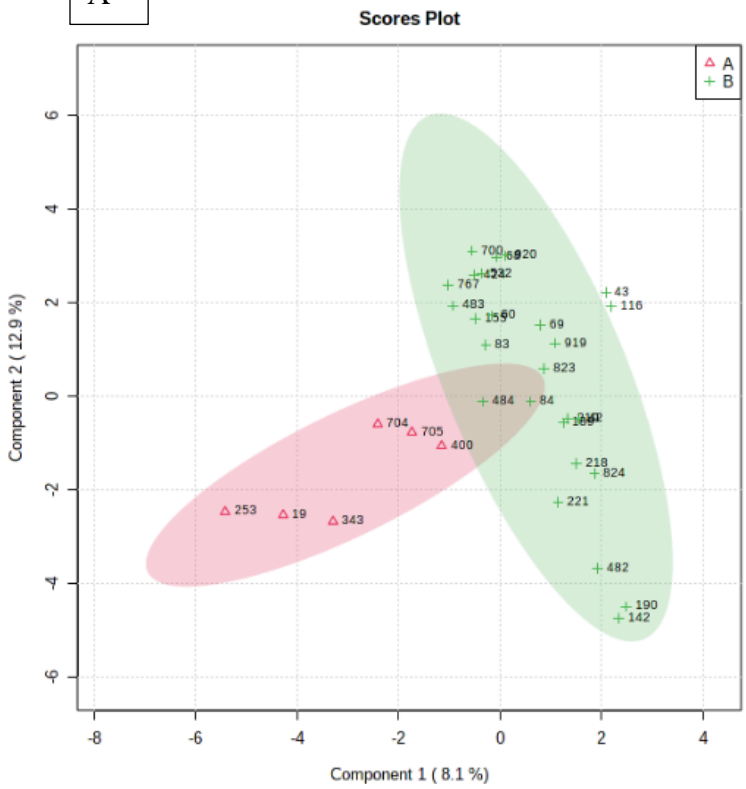

Legend in next page

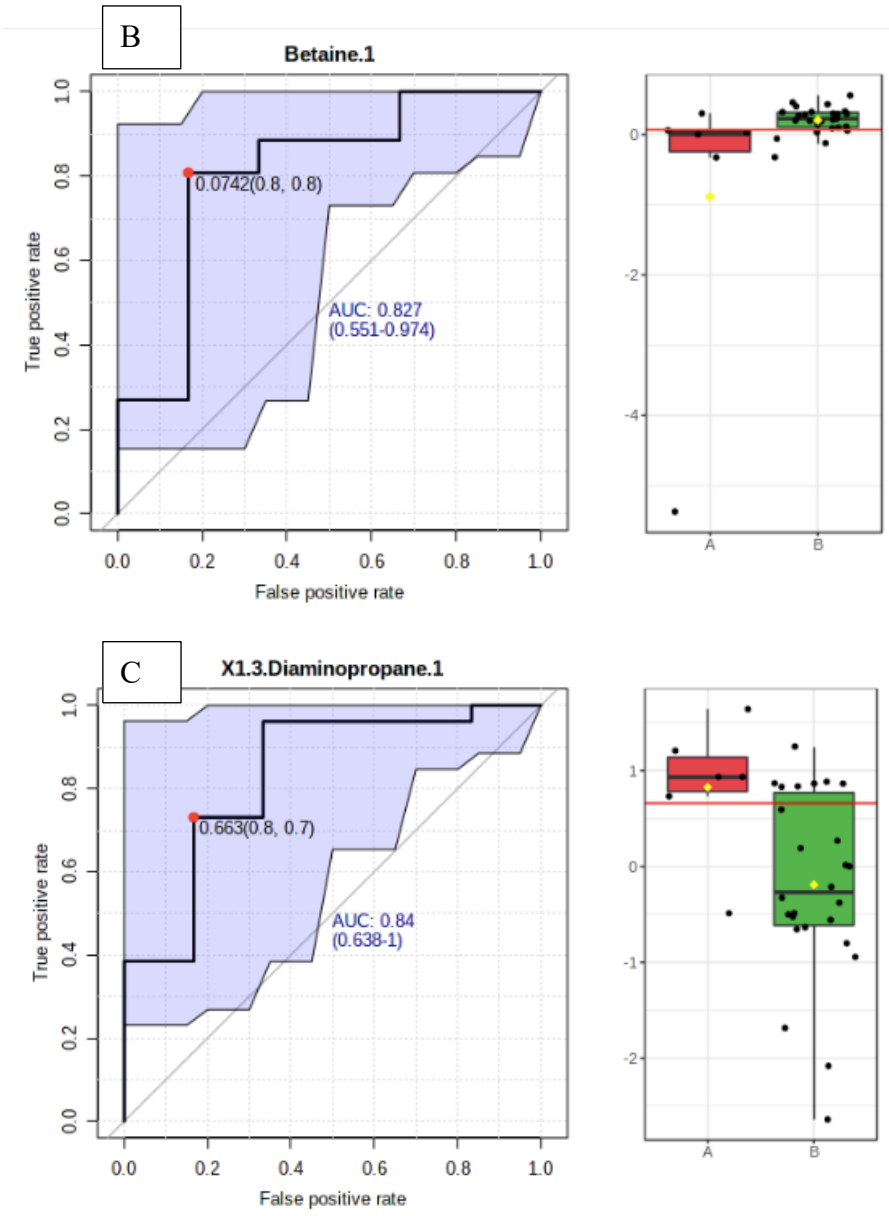
B
Betaine.1
0.0742(0.8, 0.8)
AUC: 0.827
(0.551-0.974)
True positive rate
False positive rate
0.0
0.2
0.4
0.6
0.8
1.0
0
-2
-4
A
B
C
X1.3.Diaminopropane.1
0.663(0.8, 0.7)
AUC: 0.84
(0.638-1)
True positive rate
False positive rate
1
0
-1
-2

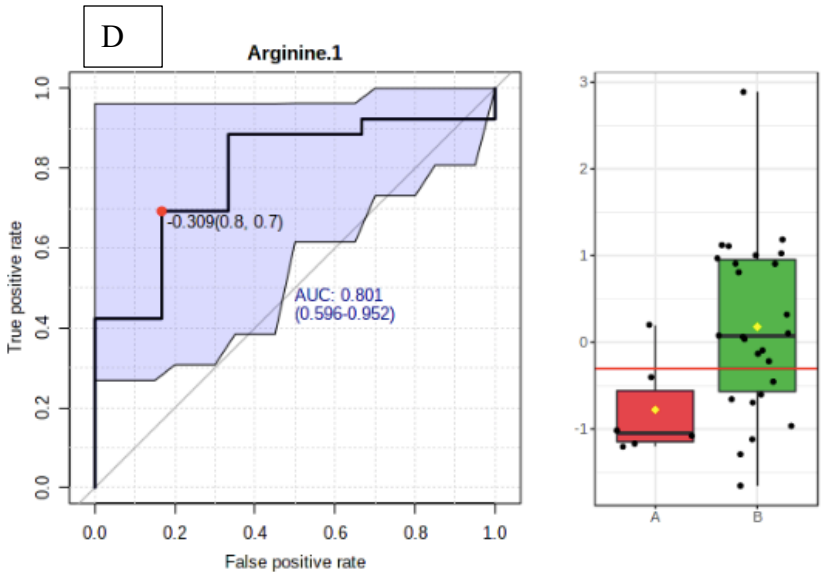

Figure 17. Significant metabolites showing separation between progressors and healthy groups. (A) PLS-DA plot comparing progressors (group A, red) with healthy implants (group B, green) demonstrating a tight grouping of metabolites separating the groups, yet statistical significance was not reached. **(B-D)** High accuracy in the ROC analysis was demonstrated by 1-3-diaminopropane showing correlation with the progressors (AUC= 0.84) while betaine and arginine were correlated with healthy implants (AUC= 0.827 and 0.801 respectively). The blue band represents the 95% confidence interval while the solid red dot indicates the optimal cutoff with the associated sensitivity and specificity values.

6 DISCUSSION

6.1 Standardizing study design for peri-implantitis

There was a wide heterogeneity in defining PI. We defined PI according to the “2017 World Workshop on the Classification of Periodontal and Peri-implant Diseases and Conditions” (Berglundh, Armitage et al. 2018). “In the absence of initial radiographs and probing depths, radiographic evidence of bone loss of ≥3 mm and/or probing depths ≥6 mm in conjunction with profuse bleeding fits this definition”. Peri-implant health is defined as PD ≤5.0 mm and RBL <2mm, (Araujo and Lindhe 2018). Even though the probing depth associated with peri-implant health should be ≤5.0 mm, we preferred the cut-off to be ≤4mm to allow for operator error. During the annual examiner calibration trial, exact intra-examiner and inter-examiner agreement in PD ranged between 60.7%-83.3% and 46%-66.1% respectively. The predictability increased when there was a ±1 mm leeway in measurement to be between 97.6%-100% for intra-examiner agreement and 92.1%-99.4% for inter-examiner agreement. When two examiners digitally measured the RBL on the non-indexed periapical radiographs, a paired t-test showed a significant mean difference in RBL calculations of 0.14mm ($p < 0.03$, 95% CI 0.01 to 0.28) and similar variance (SD=2.73) for both examiners. Only one examiner (H. A.) performed the RBL measurements to reduce the probability of error. A radiographic bone loss of at least 1.0 mm was considered as a cut-off for documented deterioration based on past studies recommending that “the clinical assessment for each implant monitors marginal bone loss in increments of 1.0 mm” (Misch, Perel et al. 2008, Renvert, Lindahl et al. 2012).

6.2 Metabolomics allows the discovery of novel biomarkers for diagnosis and prognosis

The composition of PICF may reflect the pathophysiology of PI. Metabolomic analysis measures small degradation molecules associated with host and bacterial metabolism. Metabolite functions include metabolism, energy storage, cell-to-cell signaling, virulence, (Vinayavekhin and Saghatelian 2010). Un-targeted Metabolomics using NMR spectroscopy can be used to both identify and quantify chemicals from the PICF in an unbiased technique similar to past studies evaluating saliva or gingival crevicular fluid around natural dentition, (Barnes, Teles et al. 2009, Barnes, Teles et al. 2010, Sugimoto, Wong et al. 2010, Barnes, Ciancio et al. 2011, Barnes, Kennedy et al. 2014, Schirra and Ford 2017, Romano, Meoni et al. 2018, Romano, Meoni et al. 2019, Yatsuoka, Ueno et al. 2019). This un-targeted approach allows the discovery of unknown biomarkers, without bias, to correlate them with PI.

Metabolomic investigations can evaluate a large collection of metabolites, which contain several promising biomarkers for risk prediction, diagnosis, and treatment effects, and present specific markers related to the outcome of interest, making it useful for clinical application. General medical metabolomic research has investigated a variety of diseases and conditions to attempt the early prediction of disease progression. For example, one recent trial found that methionine, an essential amino acid, was elevated in plasma samples in patients with short survival due to endometrial cancer with, when compared to matched patients with long survival (Strand, Tangen et al. 2019). That study concluded that specific blood metabolites were associated with poor survival rates (prognosis) with this type of cancer. Another trial mapped a “specific metabolomic profile which predicts future weight gain that is an independent predictor distinct from several other known risk factors” (Geidenstam, Hsu et al. 2019).

We identified the molecular signature of lysine in PI using unbiased metabolic profiling. This study found that simple metabolites may discriminate peri-implant health from disease. The top metabolites significantly correlated with PI were cadaverine, lysine, putrescine, alanine, tyramine, valine. While the top metabolites found correlated with implant health were alpha-

ketoglutarate, methionine and uracil. These novel metabolites may be diagnostic biomarkers for peri-implantitis.

On the other hand, in the longitudinal portion, 6 deteriorating implants (progressors: group A; containing samples from only the time point of before their largest RBL loss) were compared with healthy implants (group B; n=26) and with diseased-non-progressors (group C; n=8). The diseased-non-progressing group and the healthy group included implants that remained stable (< 0.5mm RBL change) at their following 6-month sampling (and throughout the trial period) and that did not receive any treatment either on the implant nor the teeth/implants neighboring to it. Comparing the 3 groups offered a prognostic value in forecasting implant deterioration versus stability.

The significant metabolites separating the diseased from healthy implants at baseline (cross-sectional component) were not the same metabolites showing separation in the longitudinal portion. There are two reasons why this might be. A) the diseased group at baseline included both progressors AND non-progressors, therefore the metabolomic profile is different. This trial demonstrated that not all diseased implants are equal because some progress while some are stable. Therefore, the stable (diseased-non-progressors) implants might have been incorrectly diagnosed as diseased since our diagnosis relies on RBL (which may have been historic then stabilized) and PD (which may be transient mucositis). B) The healthy implant group at baseline may have also included implants which were about to deteriorate in the near future, thus had metabolites differing from other implants which remained healthy.

6.3 Lysine, Putrescine, Cadaverine are diagnostic of peri-implantitis

Decarboxylation of amino acids may yield omega-amino acids such as beta-alanine, gamma-aminobutyrate, and delta-aminovalerate as well as alpha, omega-diamines such as putrescine and cadaverine, (Wendisch 2017). Cadaverine is a diamine formed by bacterial decarboxylation of lysine that

occurs during putrefaction of tissues. Cadaverine is almost exclusively of bacterial origin, (Barnes, Teles et al. 2009), while putrescine can be produced by both bacterial and mammalian metabolic pathways. A previous metabolomic study concluded that “both cadaverine and putrescine, the end-products of amino acid degradation, were found to be up-regulated by periodontal disease” (Barnes, Teles et al. 2009).

Lysine is an essential amino acid. Lysine degradation is related to the metabolic signatures of periodontal disease-associated microbial communities, (Sakanaka, Kuboniwa et al. 2017). Past studies link Porphyromonas gingivalis to “lysine-specific cysteine proteases”, which is also described as gingipains. Gingipains are main virulence factors with the ability to degrade immunoglobulins (IgA, IgG, IgM) (Butler, Veith et al. 2015). P. gingivalis is “a Gram-negative anaerobe considered to be a keystone pathogen in the development of the bacterial-associated inflammatory oral disease chronic periodontitis”. PI was associated with higher counts of 19 bacterial species, including P. gingivalis (Schwarz, Derks et al. 2018). Metabolites most likely and least likely to be present when Cadaverine/Lysine is present are demonstrated in **Figure 8**. This grouping may be used to develop metabolic pathways to study the physiology of implant disease.

6.4 Alpha-ketoglutarate is inversely related to peri-implantitis

This study found a strong inverse correlation between PI and alpha-ketoglutarate (α-KG), which is a key molecule in several physiologic functions such as the tricarboxylic acid cycle and is required in the production of type I collagen. Additionally, α-KG is an “immunomodulator which promotes M2 macrophage activation and T-reg (regulatory T-cell) differentiation” (Klysz, Tai et al. 2015). T-reg cells and M2 macrophages are known to regulate the immune response and play a role in inflammation resolution and repair. A recent murine study found that P. gingivalis “maintains a hyperinflammatory state by suppressing the pathway synthesis genes of α-KG” (Yu, Ding et al.

2018). The same study demonstrated that “supplementation of α-KG dramatically restored M2 activation during P. gingivalis infection”. It was concluded that this metabolite may play a role in the resolution of periodontal inflammation.

Since periodontal and peri-implant tissue breakdown involves upregulation of the immune response and destruction of Type I collagen, it is possible that α-KG’s absence from diseased peri-implant PICF in this study is a significant finding. There is a paucity of literature describing the interactions of α-KG in periodontitis and, to our knowledge, none in PI.

6.5 Proline and 1-3-diaminopropane predict future peri-implant bone loss while glucose, biotin, propionate, betaine and arginine predict implant stability

The current diagnostic criteria for peri-implantitis are clinical and radiographic signs of inflammation and bone level loss. However, there are currently no prognostic methods to guide towards the most suitable therapeutic modality. A prognostic factor is a measurement that would determine the natural progression of a specific diseased implant. This measurement, if available, would optimize the management of the patient's implant.

Analysis of variance (ANOVA) between 3 groups in this longitudinal (progressors, healthy, diseased-non-progressors) displayed statistical significance in 3 metabolites. These simple compounds may predict the short-term change in bone level around an implant. Biotin, propionate and valine exhibited a marked difference in their ratios between the groups. Biotin1 and biotin2 were significantly higher in diseased-non-progressors compared to both progressors and healthy implants ($p< 0.000$). Propionate was significantly higher in diseased-non-progressors compared to healthy ($p= 0.001$). While Valine was significantly higher in both progressors and diseased-non-progressors compared to the healthy group ($p= 0.002$). Furthermore, PICF concentrations of proline and 1-3-diaminopropane were directly proportional to progressive bone loss over time, however, the difference did not reach statistical significance possibly due to a low sample size.

Biotin, also known as vitamin B7, is an enzyme co-factor present in all cells. This metabolite was significantly higher in diseased-non-progressing implants compared to the other 2 groups. The biotin cycle "involves the utilization of biotin for covalent attachment to carboxylases and its reutilization through the release of carboxylase biotin after proteolytic degradation". Biotin deficiency may lead to unfavorable conditions which may include progressive bone loss in the case of diseased implants.

Propionate (Propionic acid) is found in humans as an end-product of the microbial digestion of carbohydrates and contribute to significant physiological activities. These gut microbes include Bacteroides, Clostridium, Dialister, Megasphaera, Phascolarctobacterium, Propionibacterium, Propionigenum, Salmonella, Selenomonas and Veillonella. Propionate was significantly higher in diseased-non-progressors compared to healthy implants.

Valine was significantly higher in both progressors and diseased-non-progressors compared to the healthy group. Valine is an essential amino acid named after the plant valerian. It is critical for human life and has a role in stress and energy metabolism. This metabolite, when analyzed in the saliva, was found to be biomarker for pancreatic cancer in a metabolomics study (Sugimoto, Wong et al. 2010). Increased levels of valine were found in saliva samples of individuals with moderate-severe periodontitis (Liebsch, Pitchika et al. 2019). This amino-acid's catabolism provides energy for bacteria and its pathway was found in periodontal pathogenic P. gingivalis, Prevotella intermedia, Eubayterium brachy.

Other metabolites' differences did not reach statistical difference in the ANOVA analysis, however, displayed high accuracy in the ROC analysis. Proline and 1-3-diaminopropane were higher in the progressors (AUC= 0.917 and 0.854 respectively). While Glucose was correlated with the diseased-non-progressors (AUC= 0.896). An AUC value of 0.9 or more is considered excellent in accuracy while a value of 0.8 – 0.9 demonstrates good accuracy for this biomarker while a value of 0.7 – 0.8 is fair. However, a value of 0.6 – 0.7 is considered poor while a value between 0.5 – 0.6 is considered a failed predictive biomarker. Proline offered an excellent accuracy in predicting disease progression while 1-3-diaminopropane demonstrated a good accuracy.

Proline is an essential component of collagen and was recently found to be associated with more severely affected periodontal disease in a salivary metabolomics study (Marchesan, Morelli et al. 2015, Bostanci, Grant et al. 2021). Therefore, this metabolite's association with progressive peri-implant disease in this study was not surprising. Additionally, 1-3-Diaminopropane

was associated with the progressors group compared to both other groups. This metabolite is a toxic monoalkylamine, however, it is present in certain foods such as certain mushrooms, grapes and cinnamon. It is involved in the arginine/proline metabolic pathways and the beta-alanine metabolism. This metabolite, 1-3-Diaminopropane, along with other urinary polyamines such as the previously mentioned putrescine and cadaverine, were previously studied and found to be markers of leukemia (Lee, Suh et al. 1998).

Although statistically insignificant, levels of arginine were inversely proportional to progressive bone loss compared to peri-implant bone level stability. Arginine levels were high in both healthy (group B) and diseased-non-progressors (group C) when compared to its low levels in the progressors group (group A). Arginine is an essential amino acid however adults are able to synthesize it in the urea cycle. Arginine and its derivatives are “key factors for inter-bacterial communication in periodontal microflora” (Sakanaka, Kuboniwa et al. 2015). “Alkali generation by oral microbes, specifically via arginine catabolic pathways, is an essential factor in maintaining plaque pH homeostasis and arginine was found to improve pH homeostasis via metabolism and microbiome modulation” (Agnello, Cen et al. 2017).

6.6 Study Limitations

Metabolomics in dentistry is still in its infancy. NMR techniques by definition, detect hydrogen resonances which in turn are matched with known molecules, yet this study had overlapping of different hydrogen resonances which are shared by different metabolites due to the limited fluid quantity sampled. Future techniques may include mass spectrometry to confirm the findings of this study. Biomarkers are not necessarily present in a single moment of PICF collection due to systemic or local factors. Therefore, longitudinal studies may confirm the concentrations of metabolites and possibly show the shifts of such concentrations in diseased implants over time or after therapy. Unfortunately, this study lacked an adequate sample size of diseased and progressing implants studied over time. This is due to the fact that most subjects with diseased implants get treatment and therefore only a handful of subjects made the decision to halt any treatment for personal reasons. Studying progressing implants may be unethical if this criterion was part of the study design. Another limitation was the use of silver membrane discs to collect PICF. Examiners found difficulty inserting these silver discs in implant crevices since implant crowns typically have a concave subgingival profile. **Figure 18** demonstrates the insertion of a pre-bent silver membrane into the implant's gingival crevice. Levels of some metabolites were under the detection limit, which may cause bias. There were no adjustments for multiple comparisons, which might be a limitation. We did not adjust for potential confounders nor batch effects, which may affect the metabolite values. The subjects and implants in each group were not matched by factors such as age, gender, smoking, periodontal disease. The findings of the current study should be verified in a larger and matched patient cohort. Being a small study cohort, the findings would not necessarily be reflected in a similar larger trials, but the current study demonstrates that metabolomics is a promising future approach when exploring biomarkers for clinical use.

6.7 Future Direction

This metabolomic study offers the first insight on simple metabolites correlating with the prognosis of peri-implantitis. The metabolomic unbiased methodology allowed the discovery of molecules which have never received focus in past PI trials. These metabolites significantly relating to peri-implant disease progression may prove influential in prognosis and the choice of therapeutic modality. Future studies may elucidate on metabolomic changes over time or after implant therapy. Additionally, metabolic pathway analysis of these relevant metabolites may explain the physiology of peri-implant disease. Since putative pathogens were found to remodel the host's metabolic pathways and upregulate inflammatory processes, it may be possible to reprogram the altered pathways through supplementation of specific metabolites.

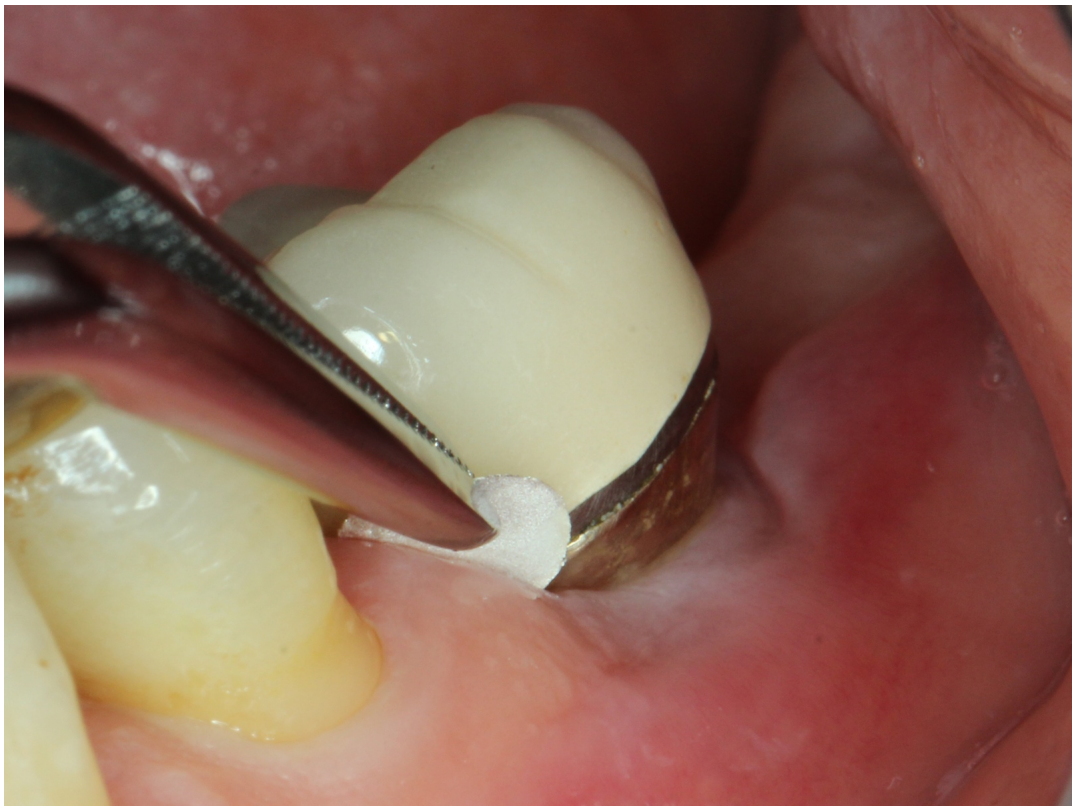

Figure 18. Insertion of a pre-bent silver membrane into the implant's gingival crevice using a cotton plier.

7 CONCLUSIONS

Peri-implant crevicular fluid (PICF) metabolites identified using proton NMR spectroscopy may be considered novel biomarkers using unbiased metabolomic profiling. These metabolomic profiles were able to discriminate between peri-implantitis and healthy implants as well as for early detection of disease progression. Lysine coherent resonances were significantly correlated with peri-implantitis while alpha-ketoglutarate was correlated with implant health. Furthermore, profiles of biotin, propionate and valine exhibited statistically significant differences when comparing the implants which had progressive bone loss over time with implants having non-progressing peri-implantitis and with healthy implants. This study also identified the molecular signatures of proline and 1-3-diaminopropane in peri-implantitis progression, while arginine was associated with non-progressing peri-implantitis, however, statistical significance was not reached. Future studies may investigate the metabolic pathways of these metabolites associated with peri-implantitis and its progression to better understand its pathogenesis and biological mechanisms. This knowledge may assist in the diagnosis and predict the disease progression of peri-implantitis.

8 BIBLIOGRAPHY

Agnello, M., L. Cen, N. C. Tran, W. Shi, J. S. McLean and X. He (2017). "Arginine Improves pH Homeostasis via Metabolism and Microbiome Modulation." J Dent Res **96**(8): 924-930.

Al-Ani, B., M. Fitzpatrick, H. Al-Nuaimi, A. M. Coughlan, F. B. Hickey, C. D. Pusey, C. Savage, C. M. Benton, E. C. O'Brien, D. O'Toole, K. H. Mok, S. P. Young and M. A. Little (2016). "Changes in urinary metabolomic profile during relapsing renal vasculitis." Sci Rep **6**: 38074.

Almehmadi, A. H. and F. Alghamdi (2018). "Biomarkers of alveolar bone resorption in gingival crevicular fluid: A systematic review." Arch Oral Biol **93**: 12-21.

Arakawa, H., J. Uehara, E. S. Hara, W. Sonoyama, A. Kimura, M. Kanyama, Y. Matsuka and T. Kuboki (2012). "Matrix metalloproteinase-8 is the major potential collagenase in active peri-implantitis." J Prosthodont Res **56**(4): 249-255.

Araujo, M. G. and J. Lindhe (2018). "Peri-implant health." J Periodontol **89 Suppl 1**: S249-s256.

Arikan, F., N. Buduneli and N. Kutukculer (2008). "Osteoprotegerin levels in peri-implant crevicular fluid." Clin Oral Implants Res **19**(3): 283-288.

Arikan, F., N. Buduneli and D. F. Lappin (2011). "C-telopeptide pyridinoline crosslinks of type I collagen, soluble RANKL, and osteoprotegerin levels in crevicular fluid of dental implants with peri-implantitis: a case-control study." Int J Oral Maxillofac Implants **26**(2): 282-289.

Atieh, M. A., J. K. Pang, K. Lian, S. Wong, A. Tawse-Smith, S. Ma and W. J. Duncan (2019). "Predicting peri-implant disease: Chi-square automatic interaction detection (CHAID) decision tree analysis of risk indicators." J Periodontol **90**(8): 834-846.

Barnes, V. M., S. G. Ciancio, O. Shibly, T. Xu, W. Devizio, H. M. Trivedi, L. Guo and T. J. Jonsson (2011). "Metabolomics reveals elevated macromolecular degradation in periodontal disease." J Dent Res **90**(11): 1293-1297.

Barnes, V. M., A. D. Kennedy, F. Panagakos, W. Devizio, H. M. Trivedi, T. Jonsson, L. Guo, S. Cervi and F. A. Scannapieco (2014). "Global metabolomic analysis of human saliva and plasma from healthy and diabetic subjects, with and without periodontal disease." PLoS One **9**(8): e105181.

Barnes, V. M., R. Teles, H. M. Trivedi, W. Devizio, T. Xu, D. P. Lee, M. W. Mitchell, J. E. Wulff, M. V. Milburn and L. Guo (2010). "Assessment of the

effects of dentifrice on periodontal disease biomarkers in gingival crevicular fluid." J Periodontol **81**(9): 1273-1279.
Barnes, V. M., R. Teles, H. M. Trivedi, W. Devizio, T. Xu, M. W. Mitchell, M. V. Milburn and L. Guo (2009). "Acceleration of purine degradation by periodontal diseases." J Dent Res **88**(9): 851-855.
Barros, S. P., R. Williams, S. Offenbacher and T. Morelli (2016). "Gingival crevicular fluid as a source of biomarkers for periodontitis." Periodontol 2000 **70**(1): 53-64.
Basegmez, C., S. Yalcin, F. Yalcin, S. Ersanli and E. Mijiritsky (2012). "Evaluation of periimplant crevicular fluid prostaglandin E2 and matrix metalloproteinase-8 levels from health to periimplant disease status: a prospective study." Implant Dent **21**(4): 306-310.
Berglundh, T., G. Armitage, M. G. Araujo, G. Avila-Ortiz, J. Blanco, P. M. Camargo, S. Chen, D. Cochran, J. Derks, E. Figuero, C. H. F. Hammerle, L. J. A. Heitz-Mayfield, G. Huynh-Ba, V. Iacono, K. T. Koo, F. Lambert, L. McCauley, M. Quirynen, S. Renvert, G. E. Salvi, F. Schwarz, D. Tarnow, C. Tomasi, H. L. Wang and N. Zitzmann (2018). "Peri-implant diseases and conditions: Consensus report of workgroup 4 of the 2017 World Workshop on the Classification of Periodontal and Peri-Implant Diseases and Conditions." J Periodontol **89 Suppl 1**: S313-s318.
Bevilacqua, L., M. D. Biasi, M. G. Lorenzon, C. Frattini and D. Angerame (2016). "Volumetric Analysis of Gingival Crevicular Fluid and Peri-Implant Sulcus Fluid in Healthy and Diseased Sites: A Cross-Sectional Split-Mouth Pilot Study." Open Dent J **10**: 131-138.
Bhavsar, I., C. S. Miller, J. L. Ebersole, D. R. Dawson, 3rd, K. L. Thompson and M. Al-Sabbagh (2019). "Biological response to peri-implantitis treatment." J Periodontal Res.
Bostanci, N., M. Grant, K. Bao, A. Silbereisen, F. Hetrodt, D. Manoil and G. N. Belibasakis (2021). "Metaproteome and metabolome of oral microbial communities." Periodontol 2000 **85**(1): 46-81.
Butler, C. A., P. D. Veith, M. F. Nieto, S. G. Dashper and E. C. Reynolds (2015). "Lysine acetylation is a common post-translational modification of key metabolic pathway enzymes of the anaerobe Porphyromonas gingivalis." J Proteomics **128**: 352-364.
Cakal, O. T., C. Efeoglu and E. Bozkurt (2018). "The evaluation of peri-implant sulcus fluid osteocalcin, osteopontin, and osteonectin levels in peri-implant diseases." J Periodontol **89**(4): 418-423.
Califf, K. J., K. Schwarzberg-Lipson, N. Garg, S. M. Gibbons, J. G. Caporaso, J. Slots, C. Cohen, P. C. Dorrestein and S. T. Kelley (2017). "Multi-omics Analysis

of Periodontal Pocket Microbial Communities Pre- and Posttreatment." mSystems **2**(3).
Carcuac, O. and T. Berglundh (2014). "Composition of human peri-implantitis and periodontitis lesions." J Dent Res **93**(11): 1083-1088.
Casado, P. L., L. Canullo, A. de Almeida Filardy, J. M. Granjeiro, E. P. Barboza and M. E. Leite Duarte (2013). "Interleukins 1beta and 10 expressions in the periimplant crevicular fluid from patients with untreated periimplant disease." Implant Dent **22**(2): 143-150.
Chatzopoulos, G. S., K. C. Mansky, S. Lunos, M. Costalonga and L. F. Wolff (2019). "Sclerostin and WNT-5a gingival protein levels in chronic periodontitis and health." J Periodontal Res **54**(5): 555-565.
Chong, J., D. S. Wishart and J. Xia (2019). "Using MetaboAnalyst 4.0 for Comprehensive and Integrative Metabolomics Data Analysis." Curr Protoc Bioinformatics **68**(1): e86.
Costalonga, M. and M. C. Herzberg (2014). "The oral microbiome and the immunobiology of periodontal disease and caries." Immunol Lett **162**(2 Pt A): 22-38.
Delima, A. J. and T. E. Van Dyke (2003). "Origin and function of the cellular components in gingival crevice fluid." Periodontol 2000 **31**: 55-76.
Derks, J., D. Schaller, J. Hakansson, J. L. Wennstrom, C. Tomasi and T. Berglundh (2016). "Peri-implantitis - onset and pattern of progression." J Clin Periodontol **43**(4): 383-388.
Derks, J. and C. Tomasi (2015). "Peri-implant health and disease. A systematic review of current epidemiology." J Clin Periodontol **42 Suppl 16**: S158-171.
Duarte, P. M., A. C. de Mendonca, M. B. Maximo, V. R. Santos, M. F. Bastos and F. H. Nociti (2009). "Effect of anti-infective mechanical therapy on clinical parameters and cytokine levels in human peri-implant diseases." J Periodontol **80**(2): 234-243.
Duarte, P. M., C. R. Serrao, T. S. Miranda, L. C. Zanatta, M. F. Bastos, M. Faveri, L. C. Figueiredo and M. Feres (2016). "Could cytokine levels in the peri-implant crevicular fluid be used to distinguish between healthy implants and implants with peri-implantitis? A systematic review." J Periodontal Res **51**(6): 689-698.
Dursun, E. and T. F. Tozum (2016). "Peri-Implant Crevicular Fluid Analysis, Enzymes and Biomarkers: a Systemetic Review." J Oral Maxillofac Res **7**(3): e9.
Eckert, M., D. Mizgalska, A. Sculean, J. Potempa, A. Stavropoulos and S. Eick (2018). "In vivo expression of proteases and protease inhibitor, a serpin, by periodontal pathogens at teeth and implants." Mol Oral Microbiol **33**(3): 240-248.
El Khouli, R. H., K. J. Macura, P. B. Barker, M. R. Habba, M. A. Jacobs and D. A. Bluemke (2009). "Relationship of temporal resolution to diagnostic

performance for dynamic contrast enhanced MRI of the breast." J Magn Reson Imaging **30**(5): 999-1004.
Elani, H. W., J. R. Starr, J. D. Da Silva and G. O. Gallucci (2018). "Trends in Dental Implant Use in the U.S., 1999-2016, and Projections to 2026." J Dent Res **97**(13): 1424-1430.
Englezos, E., J. Cosyn, S. Koole, W. Jacquet and H. De Bruyn (2018). "Resective Treatment of Peri-implantitis: Clinical and Radiographic Outcomes After 2 Years." Int J Periodontics Restorative Dent **38**(5): 729-735.
Esberg, A., C. Isehed, A. Holmlund and P. Lundberg (2019). "Peri-implant crevicular fluid proteome before and after adjunctive enamel matrix derivative treatment of peri-implantitis." J Clin Periodontol **46**(6): 669-677.
Etter, T. H., I. Hakanson, N. P. Lang, P. M. Trejo and R. G. Caffesse (2002). "Healing after standardized clinical probing of the perlimplant soft tissue seal: a histomorphometric study in dogs." Clin Oral Implants Res **13**(6): 571-580.
Faot, F., G. G. Nascimento, A. M. Bielemann, T. D. Campão, F. R. M. Leite and M. Quirynen (2015). "Can Peri-Implant Crevicular Fluid Assist in the Diagnosis of Peri-Implantitis? A Systematic Review and Meta-Analysis." Journal of Periodontology **86**(5): 631-645.
Geidenstam, N., Y. H. Hsu, C. M. Astley, J. M. Mercader, M. Ridderstrale, M. E. Gonzalez, C. Gonzalez, J. N. Hirschhorn and R. M. Salem (2019). "Using metabolite profiling to construct and validate a metabolite risk score for predicting future weight gain." PLoS One **14**(9): e0222445.
Ghassib, I., Z. Chen, J. Zhu and H. L. Wang (2019). "Use of IL-1 beta, IL-6, TNF-alpha, and MMP-8 biomarkers to distinguish peri-implant diseases: A systematic review and meta-analysis." Clin Implant Dent Relat Res **21**(1): 190-207.
Gurlek, O., P. Gumus, C. J. Nile, D. F. Lappin and N. Buduneli (2017). "Biomarkers and Bacteria Around Implants and Natural Teeth in the Same Individuals." J Periodontol **88**(8): 752-761.
Hall, J., N. G. Pehrson, A. Ekestubbe, T. Jemt and B. Friberg (2015). "A controlled, cross-sectional exploratory study on markers for the plasminogen system and inflammation in crevicular fluid samples from healthy, mucositis and peri-implantitis sites." Eur J Oral Implantol **8**(2): 153-166.
Heitz-Mayfield, L. J. and N. P. Lang (2010). "Comparative biology of chronic and aggressive periodontitis vs. peri-implantitis." Periodontol 2000 **53**: 167-181.
Heitz-Mayfield, L. J. A. and G. E. Salvi (2018). "Peri-implant mucositis." Journal of Periodontology **89**(S1): S257-S266.
Kim, J. W., R. E. Wolff, P. Gaillard and L. F. Wolff (2015). "Gingival crevicular blood as a source to screen for diabetes control in a dental office setting." Am J Dent **28**(2): 63-67.

Kinney, J. S., T. Morelli, M. Oh, T. M. Braun, C. A. Ramseier, J. V. Sugai and W. V. Giannobile (2014). "Crevicular fluid biomarkers and periodontal disease progression." J Clin Periodontol **41**(2): 113-120.
Klysz, D., X. Tai, P. A. Robert, M. Craveiro, G. Cretenet, L. Oburoglu, C. Mongellaz, S. Floess, V. Fritz, M. I. Matias, C. Yong, N. Surh, J. C. Marie, J. Huehn, V. Zimmermann, S. Kinet, V. Dardalhon and N. Taylor (2015). "Glutamine-dependent alpha-ketoglutarate production regulates the balance between T helper 1 cell and regulatory T cell generation." Sci Signal **8**(396): ra97.
Kuboniwa, M., A. Sakanaka, E. Hashino, T. Bamba, E. Fukusaki and A. Amano (2016). "Prediction of Periodontal Inflammation via Metabolic Profiling of Saliva." J Dent Res **95**(12): 1381-1386.
Lee, S. H., J. W. Suh, B. C. Chung and S. O. Kim (1998). "Polyamine profiles in the urine of patients with leukemia." Cancer Lett **122**(1-2): 1-8.
Liebsch, C., V. Pitchika, C. Pink, S. Samietz, G. Kastenmuller, A. Artati, K. Suhre, J. Adamski, M. Nauck, H. Volzke, N. Friedrich, T. Kocher, B. Holtfreter and M. Pietzner (2019). "The Saliva Metabolome in Association to Oral Health Status." J Dent Res **98**(6): 642-651.
Loos, B. G. and S. Tjoa (2005). "Host-derived diagnostic markers for periodontitis: do they exist in gingival crevice fluid?" Periodontol 2000 **39**: 53-72.
Ma, J., U. Kitti, R. Hanemaaijer, O. P. Teronen, T. A. Sorsa, S. Natah, E. K. Tensing and Y. T. Konttinen (2003). "Gelatinase B is associated with peri-implant bone loss." Clin Oral Implants Res **14**(6): 709-713.
Ma, J., U. Kitti, O. Teronen, T. Sorsa, V. Husa, P. Laine, H. Ronka, T. Salo, C. Lindqvist and Y. T. Konttinen (2000). "Collagenases in different categories of peri-implant vertical bone loss." J Dent Res **79**(11): 1870-1873.
Marchesan, J. T., T. Morelli, K. Moss, S. P. Barros, M. Ward, W. Jenkins, M. B. Aspiras and S. Offenbacher (2015). "Association of Synergistetes and Cyclodipeptides with Periodontitis." J Dent Res **94**(10): 1425-1431.
Misch, C. E., M. L. Perel, H. L. Wang, G. Sammartino, P. Galindo-Moreno, P. Trisi, M. Steigmann, A. Rebaudi, A. Palti, M. A. Pikos, D. Schwartz-Arad, J. Choukroun, J. L. Gutierrez-Perez, G. Marenzi and D. K. Valavanis (2008). "Implant success, survival, and failure: the International Congress of Oral Implantologists (ICOI) Pisa Consensus Conference." Implant Dent **17**(1): 5-15.
Monov, G., G. D. Strbac, M. Baron, B. Kandler, G. Watzek and R. Gruber (2006). "Soluble RANKL in crevicular fluid of dental implants: a pilot study." Clin Implant Dent Relat Res **8**(3): 135-141.
Murata, M., J. Tatsumi, Y. Kato, S. Suda, Y. Nunokawa, Y. Kobayashi, H. Takeda, H. Araki, K. Shin, K. Okuda, T. Miyata and H. Yoshie (2002). "Osteocalcin, deoxypyridinoline and interleukin-1beta in peri-implant

crevicular fluid of patients with peri-implantitis." Clin Oral Implants Res **13**(6): 637-643.
Nomura, T., A. Ishii, H. Shimizu, N. Taguchi, H. Yoshie, H. Kusakari and K. Hara (2000). "Tissue inhibitor of metalloproteinases-1, matrix metalloproteinases-1 and -8, and collagenase activity levels in peri-implant crevicular fluid after implantation." Clin Oral Implants Res **11**(5): 430-440.
Ozeki, M., T. Nozaki, J. Aoki, T. Bamba, K. R. Jensen, S. Murakami and M. Toyoda (2016). "Metabolomic Analysis of Gingival Crevicular Fluid Using Gas Chromatography/Mass Spectrometry." Mass Spectrom (Tokyo) **5**(1): A0047.
Panagakos, F. S., H. Aboyoussef, R. Dondero and J. J. Jandinski (1996). "Detection and measurement of inflammatory cytokines in implant crevicular fluid: a pilot study." Int J Oral Maxillofac Implants **11**(6): 794-799.
Patini, R., E. Staderini, C. Lajolo, L. Lopetuso, H. Mohammed, L. Rimondini, V. Rocchetti, F. Franceschi, M. Cordaro and P. Gallenzi (2018). "Relationship between oral microbiota and periodontal disease: a systematic review." Eur Rev Med Pharmacol Sci **22**(18): 5775-5788.
Rakic, M., V. Lekovic, N. Nikolic-Jakoba, D. Vojvodic, A. Petkovic-Curcin and M. Sanz (2013). "Bone loss biomarkers associated with peri-implantitis. A cross-sectional study." Clin Oral Implants Res **24**(10): 1110-1116.
Ramseier, C. A., S. Eick, C. Bronnimann, D. Buser, U. Bragger and G. E. Salvi (2016). "Host-derived biomarkers at teeth and implants in partially edentulous patients. A 10-year retrospective study." Clin Oral Implants Res **27**(2): 211-217.
Razzouk, S. and C. Teixeira (2010). "Personalized implant therapy: new perspectives in bone remodeling assessment." N Y State Dent J **76**(4): 50-52.
Recker, E. N., G. Avila-Ortiz, C. L. Fischer, K. Pagan-Rivera, K. A. Brogden, D. V. Dawson and S. Elangovan (2015). "A cross-sectional assessment of biomarker levels around implants versus natural teeth in periodontal maintenance patients." J Periodontol **86**(2): 264-272.
Renvert, S., C. Lindahl and G. Rutger Persson (2012). "The incidence of peri-implantitis for two different implant systems over a period of thirteen years." J Clin Periodontol **39**(12): 1191-1197.
Renvert, S., G. R. Persson, F. Q. Pirih and P. M. Camargo (2018). "Peri-implant health, peri-implant mucositis, and peri-implantitis: Case definitions and diagnostic considerations." Journal of Periodontology **89**(S1): S304-S312.
Renvert, S., C. Widen and R. G. Persson (2017). "Cytokine and microbial profiles in relation to the clinical outcome following treatment of peri-implantitis." Clin Oral Implants Res **28**(9): 1127-1132.
Roccuzzo, M., D. M. Layton, A. Roccuzzo and L. J. Heitz-Mayfield (2018). "Clinical outcomes of peri-implantitis treatment and supportive care: A systematic review." Clin Oral Implants Res **29 Suppl 16**: 331-350.

Romano, F., G. Meoni, V. Manavella, G. Baima, G. M. Mariani, S. Cacciatore, L. Tenori and M. Aimetti (2019). "Effect of non-surgical periodontal therapy on salivary metabolic fingerprint of generalized chronic periodontitis using nuclear magnetic resonance spectroscopy." Arch Oral Biol **97**: 208-214.
Romano, F., G. Meoni, V. Manavella, G. Baima, L. Tenori, S. Cacciatore and M. Aimetti (2018). "Analysis of salivary phenotypes of generalized aggressive and chronic periodontitis through nuclear magnetic resonance-based metabolomics." J Periodontol **89**(12): 1452-1460.
Sahrmann, P., T. Attin and P. R. Schmidlin (2011). "Regenerative treatment of peri-implantitis using bone substitutes and membrane: a systematic review." Clin Implant Dent Relat Res **13**(1): 46-57.
Sakanaka, A., M. Kuboniwa, E. Hashino, T. Bamba, E. Fukusaki and A. Amano (2017). "Distinct signatures of dental plaque metabolic byproducts dictated by periodontal inflammatory status." Sci Rep **7**: 42818.
Sakanaka, A., M. Kuboniwa, H. Takeuchi, E. Hashino and A. Amano (2015). "Arginine-Ornithine Antiporter ArcD Controls Arginine Metabolism and Interspecies Biofilm Development of Streptococcus gordonii." J Biol Chem **290**(35): 21185-21198.
Schierano, G., G. Pejrone, P. Brusco, A. Trombetta, G. Martinasso, G. Preti and R. A. Canuto (2008). "TNF-alpha TGF-beta2 and IL-1beta levels in gingival and peri-implant crevicular fluid before and after de novo plaque accumulation." J Clin Periodontol **35**(6): 532-538.
Schirra, H. J. and P. J. Ford (2017). "NMR-Based Metabolomics of Oral Biofluids." Methods Mol Biol **1537**: 79-105.
Schwarz, F., J. Derks, A. Monje and H.-L. Wang (2018). "Peri-implantitis." Journal of Periodontology **89**(S1): S267-S290.
Sorsa, T., T. Tervahartiala, J. Leppilahti, M. Hernandez, J. Gamonal, A. M. Tuomainen, A. Lauhio, P. J. Pussinen and P. Mantyla (2011). "Collagenase-2 (MMP-8) as a point-of-care biomarker in periodontitis and cardiovascular diseases. Therapeutic response to non-antimicrobial properties of tetracyclines." Pharmacol Res **63**(2): 108-113.
Strand, E., I. L. Tangen, K. E. Fasmer, H. Jacob, M. K. Halle, E. A. Hoivik, B. Delvoux, J. Trovik, I. S. Haldorsen, A. Romano and C. Krakstad (2019). "Blood Metabolites Associate with Prognosis in Endometrial Cancer." Metabolites **9**(12).
Strbac, G. D., G. Monov, S. Cei, B. Kandler, G. Watzek and R. Gruber (2006). "Cathepsin K levels in the crevicular fluid of dental implants: a pilot study." J Clin Periodontol **33**(4): 302-308.
Strimbu, K. and J. A. Tavel (2010). "What are biomarkers?" Curr Opin HIV AIDS **5**(6): 463-466.

Sugimoto, M., D. T. Wong, A. Hirayama, T. Soga and M. Tomita (2010). "Capillary electrophoresis mass spectrometry-based saliva metabolomics identified oral, breast and pancreatic cancer-specific profiles." Metabolomics **6**(1): 78-95.
Tonetti, M. S., H. Greenwell and K. S. Kornman (2018). "Staging and grading of periodontitis: Framework and proposal of a new classification and case definition." J Periodontol **89 Suppl 1**: S159-s172.
Vinayavekhin, N., E. A. Homan and A. Saghatelian (2010). "Exploring disease through metabolomics." ACS Chem Biol **5**(1): 91-103.
Vinayavekhin, N. and A. Saghatelian (2010). "Untargeted metabolomics." Curr Protoc Mol Biol **Chapter 30**: Unit 30.31.31-24.
Wang, H. L., C. Garaicoa-Pazmino, A. Collins, H. S. Ong, R. Chudri and W. V. Giannobile (2016). "Protein biomarkers and microbial profiles in peri-implantitis." Clin Oral Implants Res **27**(9): 1129-1136.
Wendisch, V. F. (2017). "Microbial Production of Amino Acid-Related Compounds." Adv Biochem Eng Biotechnol **159**: 255-269.
Wishart, D. S. (2008). "Quantitative metabolomics using NMR." TrAC Trends in Analytical Chemistry **27**(3): 228-237.
Wohlfahrt, J. C., A. M. Aass, F. Granfeldt, S. P. Lyngstadaas and J. E. Reseland (2014). "Sulcus fluid bone marker levels and the outcome of surgical treatment of peri-implantitis." J Clin Periodontol **41**(4): 424-431.
Wolff, L., G. Dahlen and D. Aeppli (1994). "Bacteria as Risk Markers for Periodontitis." J Periodontol **65 Suppl 5S**: 498-510.
Wolff, L. F., Q. T. Smith, W. K. Snyder, J. A. Bedrick, W. F. Liljemark, D. A. Aeppli and C. L. Bandt (1988). "Relationship between lactate dehydrogenase and myeloperoxidase levels in human gingival crevicular fluid and clinical and microbial measurements." J Clin Periodontol **15**(2): 110-115.
Xu, L., Z. Yu, H. M. Lee, M. S. Wolff, L. M. Golub, T. Sorsa and H. Kuula (2008). "Characteristics of collagenase-2 from gingival crevicular fluid and peri-implant sulcular fluid in periodontitis and peri-implantitis patients: pilot study." Acta Odontol Scand **66**(4): 219-224.
Yamalik, N., S. Gunday, S. Uysal, K. Kilinc, E. Karabulut and T. F. Tozum (2012). "Analysis of cathepsin-K activity at tooth and dental implant sites and the potential of this enzyme in reflecting alveolar bone loss." J Periodontol **83**(4): 498-505.
Yatsuoka, W., T. Ueno, K. Miyano, Y. Uezono, A. Enomoto, M. Kaneko, S. Ota, T. Soga, M. Sugimoto and T. Ushijima (2019). "Metabolomic profiling reveals salivary hypotaurine as a potential early detection marker for medication-related osteonecrosis of the jaw." PLoS One **14**(8): e0220712.

Yu, S., L. Ding, D. Liang and L. Luo (2018). "Porphyromonas gingivalis inhibits M2 activation of macrophages by suppressing alpha-ketoglutarate production in mice." Mol Oral Microbiol **33**(5): 388-395.
Zani, S. R., K. Moss, J. A. Shibli, E. R. Teixeira, R. de Oliveira Mairink, T. Onuma, M. Feres and R. P. Teles (2016). "Peri-implant crevicular fluid biomarkers as discriminants of peri-implant health and disease." J Clin Periodontol **43**(10): 825-832.